

**Synthesis and Characterization of
Platinum(II)–Bis(boryl) Catalyst Precursors for
Diboration of Alkynes and Diynes: Molecular Structures
of *cis*-[(PPh₃)₂Pt(B-4-Bu^tcat)₂], *cis*-[(PPh₃)₂Pt(Bcat)₂],
cis-[(dppe)Pt(Bcat)₂], *cis*-[(dppb)Pt(Bcat)₂],
(*E*)-(4-MeOC₆H₄)C(Bcat)=CH(Bcat),
(*Z*)-(C₆H₅)C(Bcat)=C(C₆H₅)(Bcat), and
(*Z,Z*)-(4-MeOC₆H₄)C(Bcat)=C(Bcat)C(Bcat)=C(4-MeOC₆H₄)(Bcat)
(cat = 1,2-O₂C₆H₄; dppe = Ph₂PCH₂CH₂PPh₂; dppb =
Ph₂P(CH₂)₄PPh₂)**

Gerry Lesley, Paul Nguyen, Nicholas J. Taylor, and Todd B. Marder*

Department of Chemistry, University of Waterloo, Waterloo, Ontario N2L 3G1, Canada

Andrew J. Scott, William Clegg, and Nicholas C. Norman*,†

*Department of Chemistry, University of Newcastle-upon-Tyne,
Newcastle-upon-Tyne NE1 7RU, England*

Received November 28, 1995[⊗]

The reactions of the B–B-bonded compounds B₂(cat)₂ (cat = 1,2-O₂C₆H₄) (**1a**), B₂(4-Bu^tcat)₂ (**1b**), and B₂(OCMe₂CMe₂O)₂ (**1c**) with the Pt(0)-bis(phosphine) complex [(PPh₃)₂Pt(η-C₂H₄)] (**4**) via oxidative addition of the B–B bond yield *cis*-bis(boryl) Pt(II) complexes. The molecular structures of *cis*-[(PPh₃)₂Pt(Bcat)₂]·C₆D₆ (**3a**) and *cis*-[(PPh₃)₂Pt(B-4-Bu^tcat)₂] (**3b**) were determined by single-crystal X-ray diffraction. Reaction of **3a** with 1 equiv of the bidentate phosphine dppe (Ph₂PCH₂CH₂PPh₂) or dppb (Ph₂P(CH₂)₄PPh₂) proceeds smoothly in toluene to give *cis*-[(dppe)Pt(Bcat)₂] (**5a**) and *cis*-[(dppb)Pt(Bcat)₂] (**5b**), respectively, which have also been characterized by X-ray diffraction. Compounds **3a**, **b** and **4** are highly active catalyst precursors for the diboration of alkynes and 1,3-diynes. X-ray crystal structures of (*E*)-(4-MeOC₆H₄)C(Bcat)=CH(Bcat) (**10c**), (*Z*)-(C₆H₅)C(Bcat)=C(C₆H₅)(Bcat) (**10e**), and (*Z,Z*)-(4-MeOC₆H₄)C(Bcat)=C(Bcat)C(Bcat)=C(4-MeOC₆H₄)(Bcat) (**14a**) confirm the *cis* stereochemistry of the boron substituents in three representative cases, namely, products of the catalyzed diboration of the terminal alkyne 4-MeOC₆H₄C≡CH, the internal alkyne PhC≡CPh, and the tetraboration of the diyne 4,4'-MeOC₆H₄C≡CC≡CC₆H₄OMe. The presence of the C≡CSiMe₃ moiety in catalytic reactions gives rise to additional products other than those derived from the diboration of the alkyne group. Metathetical reactions involving the diboron reagent and products derived from C–Si bond cleavage give rise to novel tris(boronate esters) as a result of the subsequent diboration of the C≡CB(OR)₂ moieties formed by this competing process. The absence of catalytic activity using compound **5a**, the extremely low activity of **5b**, and the strong decrease in activity of **3b** in the presence of added PPh₃ suggests that phosphine dissociation is a critical step in the catalytic pathway.

Introduction

While metal-catalyzed alkene hydroboration has received much attention¹ in recent years, studies of the

catalytic addition of B–B bonds to alkenes² and alkynes³ have only just begun to appear. The diboron tetrahalides B₂X₄ (X = F, Cl, Br) add readily across C–C multiple bonds in the absence of a catalyst; however, difficulties with the preparation and isolation of these reagents present considerable drawbacks for routine use.⁴ We have recently reported⁵ the oxidative addition of B–B bonds in B₂(OR)₄ ((OR)₂ = cat = 1,2-O₂C₆H₄ (**1a**); (OR)₂ = 4-Bu^tcat = 1,2-O₂-4-Bu^tC₆H₃ (**1b**)) compounds

* Present address: University of Bristol, School of Chemistry, Bristol BS8 1TS, England.

[⊗] Abstract published in *Advance ACS Abstracts*, June 1, 1996.

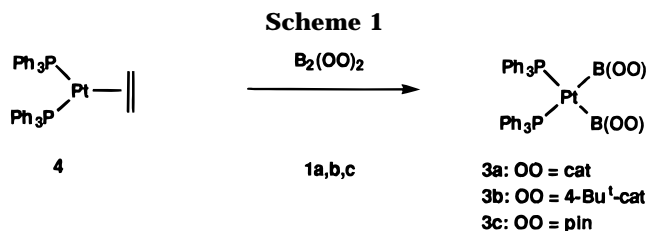
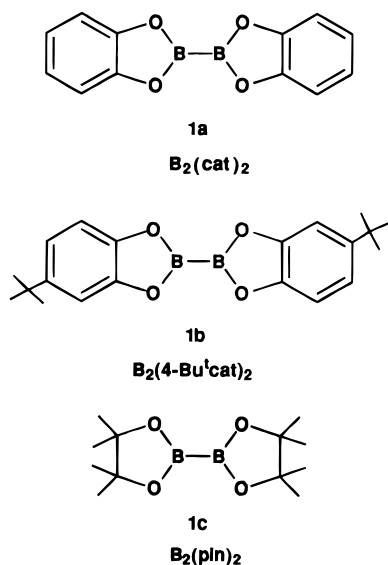
(1) For leading references, see: (a) Männig, D.; Nöth, H. *Angew. Chem., Int. Ed. Engl.* **1985**, *24*, 878. (b) Burgess, K.; Ohlmeyer, M. *J. Chem. Rev.* **1991**, *91*, 1179. (c) Evans, D.; Fu, G. C. *J. Am. Chem. Soc.* **1992**, *114*, 6679. (d) Gridnev, I. D.; Miyaura, N.; Suzuki, A. *J. Org. Chem.* **1993**, *58*, 5351. (e) Brown, J.; Lloyd-Jones, G. C. *J. Am. Chem. Soc.* **1994**, *116*, 866. (f) Matsumoto, Y.; Naito, M.; Uozumi, Y.; Hayashi, T. *J. Chem. Soc., Chem. Commun.* **1993**, 1468. (g) Hou, X.; Hong, D.; Rong, G.; Guo, Y.; Dai, L. *Tetrahedron Lett.* **1993**, *34*, 8513. (h) Westcott, S. A.; Blom, H. P.; Marder, T. B.; Baker, R. T. *J. Am. Chem. Soc.* **1992**, *114*, 8863. (i) Burgess, K.; Van der Donk, W. A.; Westcott, S. A.; Marder, T. B.; Baker, R. T.; Calabrese, J. C. *J. Am. Chem. Soc.* **1992**, *114*, 9350. (j) Harrison, K. N.; Marks, T. J. *J. Am. Chem. Soc.* **1992**, *114*, 9220. (k) Pereira, S.; Srebnik, M. *Organometallics* **1995**, *14*, 3127.

(2) Baker, R. T.; Nguyen, P.; Marder, T. B.; Westcott, S. A. *Angew. Chem., Int. Ed. Engl.* **1995**, *34*, 1336.

(3) (a) Ishiyama, T.; Matsuda, N.; Miyaura, N.; Suzuki, A. *J. Am. Chem. Soc.* **1993**, *115*, 11018. (b) Ishiyama, T.; Matsuda, N.; Murata, M.; Ozawa, F.; Suzuki, A.; Miyaura, N. *Organometallics* **1996**, *15*, 713.

(4) (a) Morrison, J. A. *Chem. Rev.* **1991**, *91*, 35. (b) Massey, A. G. *Adv. Inorg. Chem. Radiochem.* **1983**, *26*, 1.

(5) Nguyen, P.; Lesley, G.; Taylor, N. J.; Marder, T. B.; Pickett, N. L.; Clegg, W.; Elsegood, M. R. J.; Norman, N. C. *Inorg. Chem.* **1994**, *33*, 4623.



than two 2 bound phosphine ligands, (2) the presence of additional phosphine might inhibit catalyst activity, and (3) $B_2(\text{cat})_2$ might show enhanced reactivity compared with $B_2(\text{pin})_2$.⁵ In this paper, we report the synthesis and characterization of a series of *cis*-bis-(phosphine)platinum(II) bis(boryl) complexes and their activity as catalyst precursors for alkyne diboration reactions.³ The effects of the nature and concentration of phosphine ligands on the catalytic activity of the Pt complexes will be discussed, as will the relative reactivity of the diboron reagents involved in these reactions.

Results and Discussion

Synthesis and Characterization of *cis*-[(R_3P)₂Pt-(boryl)₂] Compounds. Isolated samples⁹ of [(PPh₃)₂Pt(η -C₂H₄)] (**4**) react rapidly with 1.1 mol equiv of $B_2(\text{cat})_2$ (**1a**) in C₆D₆ or toluene at room temperature to give *cis*-[(PPh₃)₂Pt(Bcat)₂] (**3a**) in excellent yield (88%, based on the toluene solvate) and purity as a white precipitate (Scheme 1). Likewise, **4** reacts rapidly with **1b** to give *cis*-[(PPh₃)₂Pt(B-4-Bu^tcat)₂] (**3b**) in similar yield and purity. The yield of **3a** is greater than that previously reported (75%)^{7a} for the same reaction. Analysis of the filtrate from the reaction mixture indicates the presence of additional **3a** together with associated decomposition products (*vide infra*). This indicates that the reaction is nearly quantitative but that some solubility in toluene and slight decomposition in solution account for the less than 100% yields of the isolated precipitates. For compound **3b**, the enhanced solubility in toluene due to the presence of the *tert*-butyl groups is the main source for a reduction of the overall isolated yield of crystallized product from toluene. In this case the filtrate indicates the presence of **3b** with negligible decomposition over a period of 24 h. The enhanced stability of isolated **3b** vs **3a** is also observed in CDCl₃ solutions. The stoichiometric reaction (1:1.1) of **4** with $B_2(\text{pin})_2$ to form *cis*-[(PPh₃)₂Pt(Bpin)₂] (**3c**) was incomplete after stirring overnight in CDCl₃ or C₆D₆, and the products from this reaction could not be isolated due to the presence of decomposition products arising from **4** and **1c** as discussed below. The formation of **3c** was enhanced when THF was added to the reaction mixture in C₆D₆. The exact role of THF for this enhancement or shift in the equilibrium is unknown. As mentioned previously, two independent research groups have recently described synthetic routes for the isolation of **3c** with yields ranging from 70%^{7b} to 82%.^{3b}

to Rh(I) centers and have demonstrated catalyzed addition² of **1a** to styrenes using both Rh and Au catalyst precursors. We also reported⁶ that stoichiometric reactions of a Rh(III) bis(boryl) complex with alkenes gave both the expected alkyl-1,2-bis(boronate ester) diboration product as well as products derived from alkene insertion into Rh-B bonds followed by facile β -hydride elimination. Miyaura and Suzuki *et al.* first reported^{3a} NMR evidence that reactions of 10 equiv of $B_2(\text{pin})_2$ (pin = OCMe₂CMe₂O; **1c**) with [Pt(PPh₃)₄] (**2**) gave the platinum bis(boryl) complex *cis*-[(PPh₃)₂Pt(Bpin)₂] (**3c**) and that **2** is a catalyst precursor for the addition of **1c** to alkynes (24 h at 80 °C in DMF using 3 mol % of **2**). Recently, the same authors have isolated and fully characterized compound **3c** from the reaction of **2** with 20 equiv of $B_2(\text{pin})_2$.^{3b} While the present work was in progress, Iverson and Smith also reported^{7a} that [(PPh₃)₂Pt(η -C₂H₄)] (**4**) reacts with $B_2(\text{cat})_2$ with loss of ethylene, yielding *cis*-[(PPh₃)₂Pt(Bcat)₂] (**3a**), and that **3a** reacts stoichiometrically with 4-octyne in the presence of 1.5 mol equiv of $B_2(\text{cat})_2$ to give the 1,2-vinyl-bis(boronate ester) diboration product and **3a**. The metallacyclopentane [(PPh₃)₂Pt(CH₂)₄] also reacts with 2 mol equiv of $B_2(\text{cat})_2$ (8 h, 95 °C), yielding **3a** and catB(CH₂)₄Bcat. These authors have recently described the synthesis and characterization of compound **3c** by a different synthetic route requiring only stoichiometric quantities of $B_2(\text{pin})_2$.^{7b}

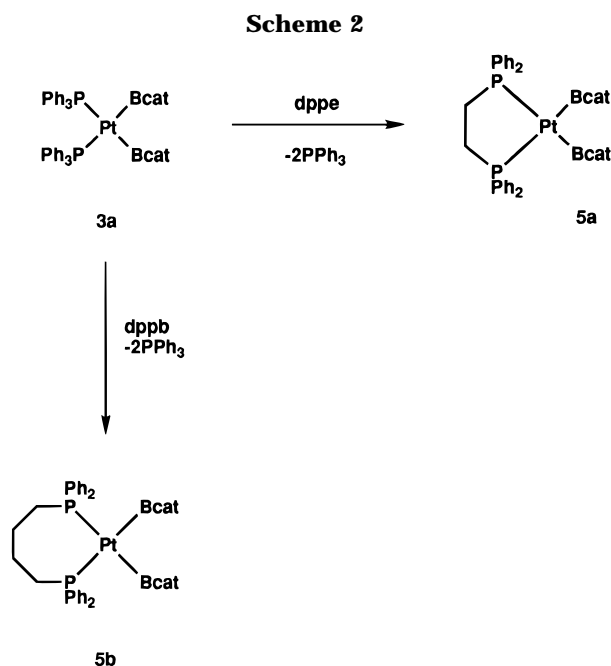
In conjunction with our studies of metal-polyboryl complexes^{5,6,8} and B-B oxidative addition to Rh(I),⁵ Co(0),^{8b} and Ir(I),^{8c} we investigated reactions of the Pt(0) complex **4** with diboron compounds **1a**–**c** and also began a study aimed at developing new diboration catalyst precursors with enhanced activities. We reasoned that (1) the active Pt catalyst was unlikely to possess more

(6) Baker, R. T.; Calabrese, J. C.; Westcott, S. A.; Nguyen, P.; Marder, T. B. *J. Am. Chem. Soc.* **1993**, *115*, 4367.

(7) (a) Iverson, C. N.; Smith, M. R., III. *J. Am. Chem. Soc.* **1995**, *117*, 4403. (b) Iverson, C. N.; Smith, M. R., III. *Organometallics*, in press.

(8) (a) Nguyen, P.; Blom, H. P.; Westcott, S. A.; Taylor, N. J.; Marder, T. B. *J. Am. Chem. Soc.* **1993**, *115*, 9329. (b) Dai, C.; Stringer, G.; Corrigan, J. F.; Taylor, N. J.; Marder, T. B.; Norman, N. C. *J. Organomet. Chem.* **1996**, *513*, 273. (c) Dai, C.; Stringer, G.; Marder, T. B.; Baker, R. T.; Scott, A. J.; Clegg, W.; Norman, N. C. *Can. J. Chem.*, in press. (d) For additional examples of metal bis(boryl) complexes see: Hartwig, J. F.; He, X. *Organometallics* **1996**, *15*, 400. (e) Cp₂W(B-4-Bu^tcat)₂ has recently been structurally characterized: Hartwig, J. F.; He, X. *Angew. Chem., Int. Ed. Engl.* **1996**, *35*, 315.

(9) Camalli, M.; Caruso, F.; Chaloupka, S.; Leber, E. M.; Rimml, H.; Venanzi, L. M. *Helv. Chim. Acta* **1990**, *73*, 2263. This paper provides a convenient synthetic route to the isolation of several bis-(phosphine)Pt(η -C₂H₄) complexes from the corresponding P₂PtCl₂ compounds. We have used the same synthetic route, with the exception that THF was substituted for CH₂Cl₂ to prepare **4**, [(dppe)Pt(η -C₂H₄)] and [(dppb)Pt(η -C₂H₄)] as isolable solids. ³¹P{¹H} NMR (81 MHz, CDCl₃): **4**, δ 34.3 ppm ($J_{\text{Pt-P}} = 3721$ Hz); [(dppe)Pt(η -C₂H₄)], δ 54.4 ppm ($J_{\text{Pt-P}} = 3303$ Hz); [(dppb)Pt(η -C₂H₄)], δ 25.5 ppm ($J_{\text{Pt-P}} = 3524$ Hz). The *in situ* preparation of [(dppe)Pt(η -C₂H₄)] has been described previously: Head, R. A. *J. Chem. Soc., Dalton Trans.* **1982**, 1637; *Inorg. Synth.* **1990**, *28*, 132 ($\delta_{\text{P}} 54.5$ ppm; $J_{\text{Pt-P}} = 3300$ Hz).



Further reaction of **3a** with 1.0 mol equiv of the bidentate phosphines dppe (1,2-bis(diphenylphosphino)ethane) and dppb (1,4-bis(diphenylphosphino)butane) in toluene at room temperature results in fine white precipitates of $\text{cis}[(\text{dppe})\text{Pt}(\text{Bcat})_2]$ (**5a**) and $\text{cis}[(\text{dppb})\text{Pt}(\text{Bcat})_2]$ (**5b**), respectively (Scheme 2). Analysis of the $^{31}\text{P}\{^1\text{H}\}$ NMR spectra of all fractions indicates clean reactions resulting in quantitative yields. As with previous results, however, some solubility of the products in toluene reduced isolated yields of **5a,b** to ca. 76–77%. Solutions of **5a** (CDCl_3 or $\text{C}_6\text{D}_6/\text{THF}$) and **5b** (CDCl_3) were stable over a period of 24 h. Alternatively, compounds **5a,b** may also be prepared by direct oxidative addition of **1a** to the corresponding $[\text{P}_2\text{Pt}(\eta\text{-C}_2\text{H}_4)]$ complexes;⁹ however, these reactions were not as clean as those described above due to impurities present from the synthesis of the Pt ethylene complexes.

Complexes **3a–c** and **5a,b** were characterized by melting point, ^1H , ^{11}B , ^{13}C , and ^{31}P NMR spectroscopy, and elemental analysis (except for **3c**) and for **3a,b** (Figures 1 and 2) and **5a,b** (Figures 3 and 4) by single-crystal X-ray diffraction. Each sample underwent a noticeable color change from white to yellow to orange prior to melting, and the temperature at which this decomposition became apparent is noted in parentheses in the Experimental Section.

The $^{31}\text{P}\{^1\text{H}\}$ NMR spectra exhibit broad resonances with $|J_{\text{Pt-P}}|$ values consistent with the *cis* coordination of the boryl ligands¹⁰ (δ_{P} 28.7, $J_{\text{Pt-P}} = 1639$ Hz, **3a**; δ_{P} 29.0, $J_{\text{Pt-P}} = 1621$ Hz, **3b**; δ_{P} 28.5, $J_{\text{Pt-P}} = 1504$ Hz, **3c**) and agree well with previously reported values for **3a** (C_6D_6 , $\delta_{\text{P}} = 30.19$, $J_{\text{Pt-P}} = 1608$ Hz)^{7a} and **3c** (toluene, δ_{P} 28.65, $J_{\text{Pt-P}} = 1517$ Hz);^{3a} however, discrepancies in the $^{11}\text{B}\{^1\text{H}\}$ NMR spectra (δ_{B} 21.5,^{3a} δ_{B} 46.3,^{3b} ca. 50 ppm (this work)) arise. We have prepared an authentic sample of $\text{B}_2(\text{pin})_3$ (**7**) which is consistent with the ^{11}B resonance reported in the initial study by Suzuki *et al.*,^{3a} as described in further detail in the section dealing with the decomposition of catalysts below. Slight deviations in $|J_{\text{Pt-P}}|$ values are expected due to the broadness of

the resonances, which is apparently due to strong coupling with the quadrupolar boron nuclei. The previously reported^{7a} chemical shift for **3a** is slightly different from values in this work, presumably due to solvent effects.

The ^1H NMR results are also consistent with previous values reported for **3a**. The aromatic region exhibits broad multiplets for the aryl rings in the phosphine ligand and for those associated with the 1,2-disubstituted aryl ring of the boryl ligands. In the ^1H NMR spectrum of **3b** there is coincidental overlap of two of the aromatic hydrogen atom resonances (δ 6.68 ppm, both with $J_{\text{H-H}}$ values of 1.1 Hz) associated with the boryl ligand.

The ^{13}C NMR spectra of compounds **3a** and **5a,b** exhibit similar resonances due to the Bcat ligands. The *ipso* carbon atoms resonate farthest downfield at ca. 150 ppm, and all have $^3J_{\text{Pt-C}}$ values of ca. 34 Hz (the satellites were too weak to observe for compound **5a**). The carbon atoms in the 3- and 6-positions resonate farthest upfield at ca. 110 ppm, while the resonances due to the carbon atoms in the 4- and 5-positions are slightly downfield of this at ca. 120 ppm. In the spectrum of compound **3b**, the carbon atoms in the 1- and 2-positions are inequivalent due to the *tert*-butyl substitution on the ring, and separate resonances each with $^3J_{\text{Pt-C}}$ values of 35 Hz are observed. The substitution in the 4-position also causes a downfield shift of the resonance due to the carbon atom at this position in the ring (143.2 ppm). The resonances for the *ipso* carbon of the $\text{P}(\text{C}_6\text{H}_5)_3$ ligands could not be characterized completely in all of the ^{13}C NMR spectra, due to partial overlap with the multiplets arising from the carbon atoms in the *ortho* position on the phenyl rings. As a result of this overlap, the resonances reported in the Experimental Section for compounds **3a** and **5a** are therefore not expected to be singlets but rather doublets with a slightly upfield chemical shift relative to that reported. In the spectrum of **3b**, coupling to Pt ($^2J_{\text{Pt-C}} = 20$ Hz) and P ($^1J_{\text{P-C}} = 44$ Hz) was observed for the *ipso* carbon. In the spectrum of **5a** only the coupling to P ($^1J_{\text{P-C}} = 47$ Hz) was observed.

Molecular Structure of *cis*-[(R₃P)₂Pt(boryl)₂] Compounds. In all cases, the structures of the Pt compounds display a *cis*-square-planar arrangement of the two phosphine and boryl ligands. The B(1)–B(2) distances (2.552 Å (**3a**), 2.554 Å (**3b**), 2.667 Å (**5a**), 2.514 Å (**5b**)) are large and indicate the absence of an interaction between the B atoms (B(1)–B(2) = 1.678(3) Å for **1a**⁵). In the structure of *cis*-[(PPh₃)₂Pt(Bcat)₂] (**3a**; Figure 1) the Pt–B distances average 2.049(6) Å, which is typical of third-row late-metal M–B bond lengths.^{7a,8a,c,11} The B(1)–Pt(1)–B(2) angle is considerably smaller than 90°, being 77.1(2)°, whereas the P(1)–Pt(1)–P(2) angle is 107.14(4)°. The conformations about the Pt–B bonds are such that the Bcat groups form interplanar angles of 71.3° (mean plane B(1), O(1), O(2), C(1)–C(6)) and 82.7° (mean plane B(2), O(3), O(4), C(11)–C(16)) with respect to the mean plane defined by Pt, B(1), B(2), P(1), P(2).

(11) (a) Knorr, J. R.; Merola, J. S. *Organometallics* **1990**, *9*, 3008. (b) Baker, R. T.; Ovenall, D. W.; Calabrese, J. C.; Westcott, S. A.; Taylor, N. J.; Williams, I. D.; Marder, T. B. *J. Am. Chem. Soc.* **1990**, *112*, 9399. (c) Lu, Z.; Jun, C.-H.; de Gala, S. R.; Sigalas, M.; Eisenstein, O.; Crabtree, R. H. *J. Chem. Soc., Chem. Commun.* **1993**, 1877. (d) Westcott, S. A.; Marder, T. B.; Baker, R. T.; Calabrese, J. C. *Can. J. Chem.* **1993**, *71*, 930.

(10) The authors in refs 3a and 7a have discussed this issue in terms of related Pt bis(silyl) complexes and the *trans* effect of the Bcat group, respectively.

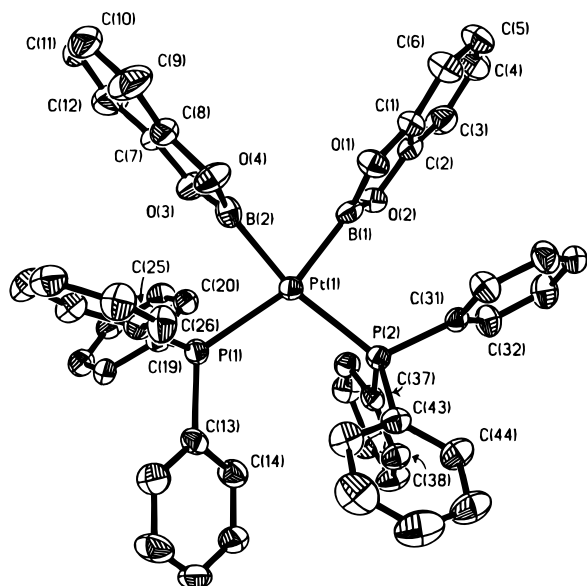


Figure 1. Molecular structure of *cis*-[(PPh₃)₂Pt(B(1,2-O₂C₆H₄))₂] (**3a**), with 50% probability ellipsoids.

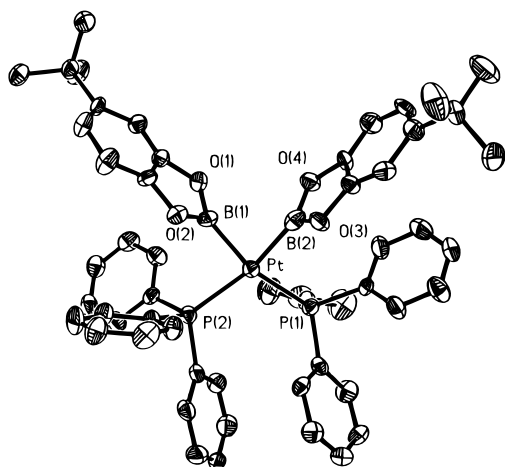


Figure 2. Molecular structure of *cis*-[(PPh₃)₂Pt(B(1,2-O₂-4-Bu^tC₆H₄))₂] (**3b**), with 50% probability ellipsoids.

The structure of *cis*-[(PPh₃)₂Pt(B(4-Bu^tcat))₂] (**3b**; Figure 2) is very similar to that of **3a**. The Pt–B distances average 2.046(13) Å, and the B(1)–Pt(1)–B(2) angle is also considerably smaller than 90°, being 77.2(4)°, while the P(1)–Pt(1)–P(2) angle is 104.37(10)°. The B(4-Bu^tcat) groups form interplanar angles of 75.9° (mean plane B(1), O(1), O(2), C(1)–C(6)) and 86.7° (mean plane B(2), O(3), O(4), C(11)–C(16)) with respect to the mean plane defined by Pt, B(1), B(2), P(1), P(2).

In the structure of *cis*-[(dppe)Pt(Bcat)₂] (**5a**; Figure 3), the Pt–B distances average 2.053(8) Å, similar to **3a,b**, but the B(1)–Pt(1)–B(2) angle is opened to 81.0(3)°, concomitant with the P(1)–Pt(1)–P(2) angle being reduced to 85.36(6)° due to the presence of the five-membered chelate ring. The conformations about the Pt–B bonds are also rather different from those observed for **3a,b** such that the Bcat groups form interplanar angles of 55.1° (mean plane B(1), O(1), O(2), C(1)–C(6)) and 88.8° (mean plane B(2), O(3), O(4), C(11)–C(16)) with respect to the mean plane defined by Pt, B(1), B(2), P(1), P(2).

In the structure of *cis*-[(dppb)Pt(Bcat)₂] (**5b**; Figure 4), the Pt–B distances are both 2.031(8) Å, the B(1)–Pt(1)–B(2) angle is reduced to 76.5(4)°, concomitant with the P(1)–Pt(1)–P(2) angle opening to 100.72(9)°,

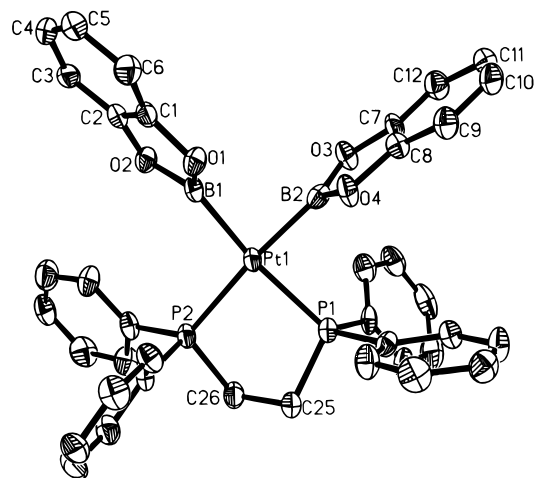


Figure 3. Molecular structure of *cis*-[(Ph₂PCH₂CH₂PPh₂)-Pt(B(1,2-O₂C₆H₄))₂] (**5a**), with 50% probability ellipsoids.

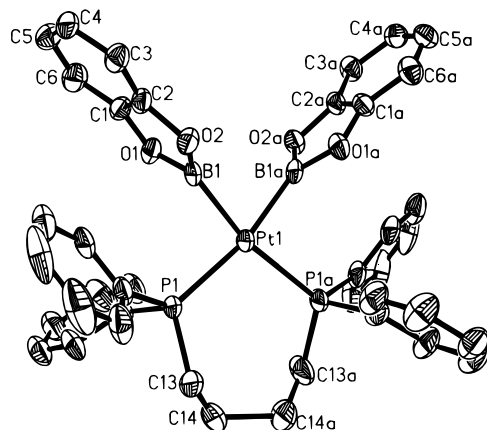


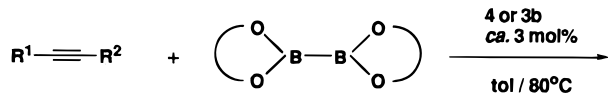
Figure 4. Molecular structure of *cis*-[(Ph₂P(CH₂)₄PPh₂)-Pt(B(1,2-O₂C₆H₄))₂] (**5b**), with 50% probability ellipsoids.

and the structure is therefore more similar to **3a,b** than to **5a**. The conformations about the Pt–B bonds are also more similar to **3a,b** than to **5a** in that the Bcat groups form interplanar angles of 81.4° (mean planes B(1), O(1), O(2), C(1)–C(6) and B(1a), O(1a), O(2a), C(1a)–C(6a)) with respect to the mean plane defined by Pt, B(1), B(2), P(1), P(2).

The structure of **3a** has been recently reported,^{7a} however, the results in this work provide significantly more precise structural parameters (e.g. previous values were Pt–B(1) = 2.08(2) Å, Pt–B(2) = 2.07(2) Å). In addition, while this paper was in preparation, Miyaoura *et al.*^{3b} reported the structural characterization of compound **3c**. It is interesting that the B(1)–Pt–B(2) angle is reduced even further in this structure to a value of 75.3(3)°. The Pt–B(1) and Pt–B(2) bond lengths (2.076(6) and 2.078(6) Å, respectively) are also slightly longer than those observed in this study, indicating a slight weakening of the metal–boryl bond with respect to the related catecholate derivatives.

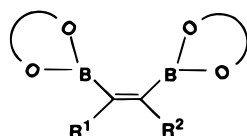
Catalytic Reactions. The catalytic activity of **3b** and **4** for the addition of B–B bonds to internal and terminal alkynes (Scheme 3) and 1,3-diyne (Scheme 4) was examined using **1a,c** and 1-octyne (**8a**), C₆H₅C≡CH (**8b**), 4-MeOC₆H₄C≡CH (**8c**), 4-NCC₆H₄C≡CH (**8d**), C₆H₅C≡CC₆H₅ (**8e**), 4-MeC₆H₄C≡CC₆H₄-4-Me (**8f**), 4-MeOC₆H₄C≡CC₆H₄-4-OMe (**8g**), Me₃SiC≡CSiMe₃ (**8h**), 4-MeOC₆H₄C≡CC≡CC₆H₄-4-OMe (**9a**), and Me₃SiC≡C–C≡CSiMe₃ (**9b**). Typical reaction conditions employed 1.9 × 10^{−4} mol of alkyne, 1.9 × 10^{−4} mol of diboron

Scheme 3



- 8a: R¹ = C₆H₁₃, R² = H
 8b: R¹ = C₆H₅, R² = H
 8c: R¹ = 4-MeO-C₆H₄, R² = H
 8d: R¹ = 4-NC-C₆H₄, R² = H
 8e: R¹ = R² = C₆H₅
 8f: R¹ = R² = 4-Me-C₆H₄
 8g: R¹ = R² = 4-MeO-C₆H₄

- 1a = B₂cat₂
 1c = B₂pin₂



- 10a: R¹ = C₆H₁₃, R² = H, OO = cat (≤3h)
 10b: R¹ = C₆H₅, R² = H, OO = cat (33h)
 10c: R¹ = 4-MeO-C₆H₄, R² = H, OO = cat (≤3h)
 10d: R¹ = 4-NC-C₆H₄, R² = H, OO = cat (≤75h)
 10e: R¹ = R² = C₆H₅, OO = cat (≤20h)
 10f: R¹ = R² = 4-Me-C₆H₄, OO = cat (≤3h)
 10g: R¹ = R² = 4-MeO-C₆H₄, OO = cat (≤3h)
 11a: R¹ = C₆H₁₃, R² = H, OO = pin (≤3h)
 11b: R¹ = C₆H₅, R² = H, OO = pin (50h)
 11c: R¹ = 4-MeO-C₆H₄, R² = H, OO = pin (≤3h)
 11d: R¹ = 4-NC-C₆H₄, R² = H, OO = pin (75h)
 11e: R¹ = R² = C₆H₅, OO = pin (≤20h)
 11f: R¹ = R² = 4-Me-C₆H₄, OO = pin (≤3h)
 11g: R¹ = R² = 4-MeO-C₆H₄, OO = pin (≤3h)

cat = 1,2-O₂C₆H₄
 pin = OCMe₂CMe₂O

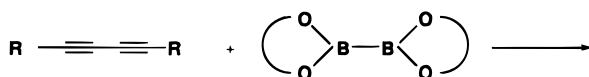
reagent (1 mol equiv), and *ca.* 5.7×10^{-6} mol (3 mol %) of catalyst in 5 mL of toluene at 80 °C. Thus, completion of the reaction constituted *ca.* 33 turnovers. Reaction progress was monitored by GC/MS using 1 μ L aliquots removed hourly from the reaction vessel. In Scheme 3, the approximate time to completion for each reaction is listed in parentheses. For **8a,c,f,g**, using either **3b** or **4**, reactions in toluene generally proceeded to completion within 3 h at 80 °C; however, for **8e** the reactions required about 20 h to reach completion. Reactions involving **8b** required extended periods of heating at 90 °C (33 h, **1a**; 50 h, **1c**) to reach completion. Using the alkyne 4-NCC₆H₄C≡CH (**8d**), reactions were incomplete after several hours and additional catalyst (7 mol % catalyst in all) and diboron reagent (*ca.* 1.5 equiv in all) were required to reach completion. A total time of 75 h at 80 °C was required. Reactions using diboron reagent **1b** were significantly slower than with **1a**, requiring, for example, >24 h for completion with alkyne **8g** at 80 °C. These results confirm our premise regarding the enhanced activity of the bis(phosphine)-platinum complexes as catalyst precursors relative to Pt(PPh₃)₄ (**2**). Both **3b** and **4** showed significantly greater activity than was reported³ for **2**, even though *all* reagents were considerably more dilute (by a factor of *ca.* 10) in our experiments when similar alkynes were employed.

The Bpin derivatives R¹C(Bpin)=C(Bpin)R² (**11a-g**) are much more soluble than the respective Bcat ana-

logues R¹C(Bcat)=C(Bcat)R² (**10a-g**) and in some cases have been isolated previously by Kugelrohr distillation.³ In this work, the products in the crude reaction mixtures were analyzed directly by NMR spectroscopy (¹H, ¹³C, and ¹¹B) and GC/MS, and both techniques were used to determine the degree of completion of the reactions. Unless otherwise stated, the reactions proceeded to 100% completion. Initial attempts to isolate the products from the scaled-up reaction (*ca.* 2 mmol of alkyne) involving **1a** and **8f** resulted in a yield of 62% of pure white solid (**10f**), which was obtained by layering the reaction mixture with hexanes. The remainder of the solids obtained (from reduction of the toluene solution and precipitation with hexanes) are slightly colored; however, NMR analysis indicates the presence of **10f** and only small amounts of impurities consistent with catalyst decomposition products. Although THF was not a suitable solvent as a reaction medium (see below), it has recently been found to be suitable for the isolation of the products. The complete separation of catalyst residue from all the pure products is currently being investigated. Compounds **10c-f**, **11g**, and **14a** have been characterized by X-ray crystallography. The single-crystal structural determinations of **10c,e** and **14a** are presented in this work; details of the structures of **10d,f** and **11g** are given elsewhere.¹²

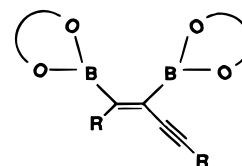
The products from the reactions of **1c** with **8a** and **8e** have been reported,³ and our spectroscopic results

Scheme 4

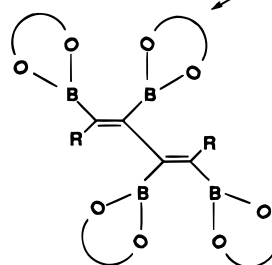


- 9a: R = 4-MeO-C₆H₄
 9b: R = SiMe₃

- 1a = B₂cat₂
 1c = B₂pin₂



- 12a: R = 4-MeO-C₆H₄; OO = cat
 12b: R = SiMe₃; OO = cat
 13a: R = 4-MeO-C₆H₄; OO = pin
 13b: R = SiMe₃; OO = pin

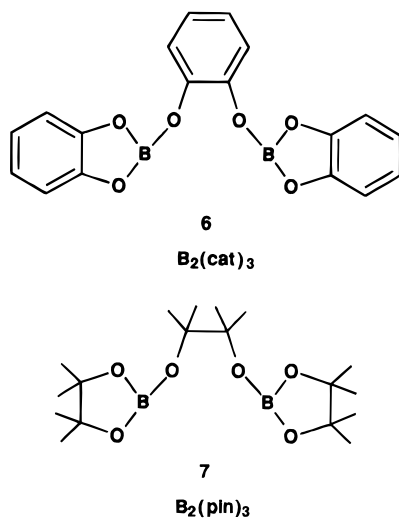


- 14a: R = 4-MeO-C₆H₄; OO = cat
 14b: R = SiMe₃; OO = cat
 15a: R = 4-MeO-C₆H₄; OO = pin
 15b: R = SiMe₃; OO = pin

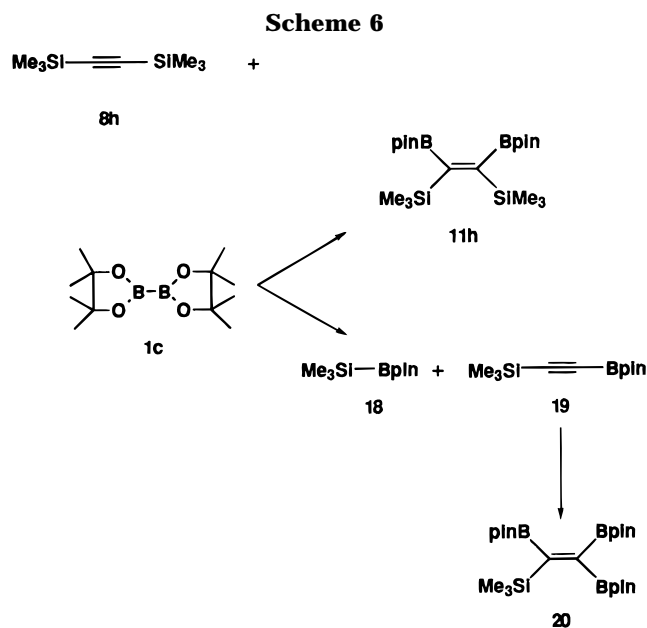
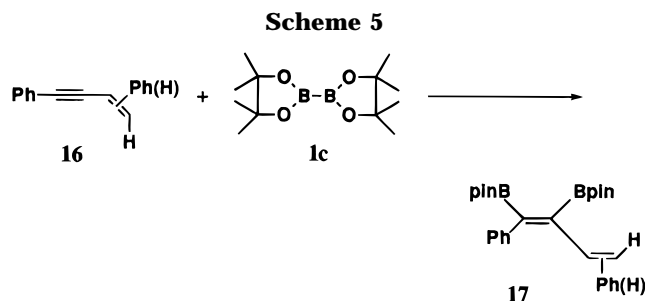
are in excellent agreement with those in the literature. The ^1H NMR spectra of **10f** in CDCl_3 obtained at 200 and 250 MHz exhibited only one broad resonance for the aromatic hydrogen atoms. In C_6D_6 , however, the resonances attributed to the chemically distinct aromatic protons were resolved at 250 MHz.

The resonances in the ^{13}C NMR spectra attributed to carbon atoms bonded directly to boron ligands were not observed in several cases, as noted in the Experimental Section. This is due to the weak, broad nature of these resonances which results from coupling with the quadrupolar boron nucleus. The broad resonances due to chemically inequivalent boron nuclei also overlap in the ^{11}B spectra of **10a–c** and **11a–c**.

As was found in previous reports,³ reactions with $\text{C}_6\text{H}_5\text{C}\equiv\text{CH}$ (**8b**) were significantly slower than for other alkynes, including 4-MeOC₆H₄C≡CH (**8c**), and likewise, in this study, those reactions involving $\text{C}_6\text{H}_5\text{C}\equiv\text{CC}_6\text{H}_5$ (**8e**) were slower than with 4-MeOC₆H₄C≡CC₆H₄OMe (**8g**). The difference in reactivity of **8b** vs **8c** and **8e** vs **8g** is no doubt a result of the differences in the electron density distributions in the C≡CH and C≡C moieties caused by the presence of the π -donor OMe group. As mentioned above, the catalytic diboration of π -acceptor-substituted 4-N≡CC₆H₄C≡CH (**8d**) with **1c** was very sluggish. The reaction was incomplete after 24 h according to GC/MS results and required a total of 7 mol % catalyst and 75 h at 80 °C to reach completion. Analysis of the ^{11}B NMR spectrum of the crude product indicated that a significant amount of $\text{B}_2(\text{pin})_3$ (**7**) had also formed. When the temperature was raised to 100 °C and 10 mol % of catalyst (**3a** for $\text{B}_2(\text{cat})_2$, **4** for $\text{B}_2(\text{pin})_2$) was employed, the reactions involving **8d** were significantly faster, requiring only 2 h to reach completion. NMR analysis of these crude reaction products using diboron reagents **1a,c** indicated that only trace amounts of $\text{B}_2(\text{cat})_3$ (**6**) and $\text{B}_2(\text{pin})_3$ (**7**) were formed, respectively.



Examination of the reactions involving the terminal alkyne $\text{C}_6\text{H}_5\text{C}\equiv\text{CH}$ (**8b**) and the internal alkyne $\text{C}_6\text{H}_5\text{C}\equiv\text{CC}_6\text{H}_5$ (**8e**) indicates that the latter reacts at a faster rate regardless of the diboron reagent used. Monitoring the reaction of **8b** with **1c** by GC/MS indicated that, in addition to the diboration product **11b**, small amounts of the butadiene–bis(boronate ester) $\text{Ph}(\text{H})\text{C}=\text{C}(\text{H})\text{C}(\text{Bpin})=\text{C}(\text{Bpin})\text{Ph}$ (**17**; configuration unknown, m/z 458 plus fragments) and the ene–yne



$\text{Ph}(\text{H})\text{C}=\text{C}(\text{H})\text{C}\equiv\text{CPh}$ (**16**; configuration unknown, m/z 204 plus fragments) were also being formed (Scheme 5). The synthesis of $[(\text{PPh}_3)_2\text{Pt}(\eta^2\text{-C}_6\text{H}_5\text{C}\equiv\text{CH})]$ has been described from both Pt(0) and Pt(II) precursors,¹³ and this compound has been shown to polymerize phenylacetylene at 130 °C.¹⁴ This would account for the formation of **16** and reduction of the observed rates when compared to reactions involving **8e**; however, the stability of the alkyne complex is probably the main source of the rate retardation observed in both cases. The presence of π -donor substituents on the phenylacetylene derivatives results in enhancement of the observed rates of reaction, presumably due to the destabilization of the $[(\text{PPh}_3)_2\text{Pt}(\eta^2\text{-alkyne})]$ or $[(\text{PPh}_3)\text{Pt}(\text{Bcat})_2(\eta^2\text{-alkyne})]$ complex (*vide infra*). In contrast, the presence of a π -acceptor substituent on the phenyl ring of the alkyne drastically reduces the observed rates of reaction, as would be expected due to the enhanced stabilization of the Pt–alkyne bond.

Interestingly, by monitoring the reaction of **8h** with **1c** using GC/MS (Scheme 6), we observed the formation of significant amounts of Me_3SiBpin (**18**) and $\text{Me}_3\text{SiC}\equiv\text{CBpin}$ (**19**), arising from C–Si bond cleavage,¹⁵ as well as the expected diboration product $\text{Me}_3\text{Si}(\text{Bpin})\text{C}=\text{C}$ –

(12) Clegg, W.; Scott, A. J.; Lesley, G.; Marder, T. B.; Norman, N. *Acta Crystallogr.*, in press.

(13) (a) Chatt, J.; Rowe, G. A.; Williams, A. A. *Proc. Chem. Soc.* **1957**, 208. (b) Greaves, E. O.; Lock, C. J. L.; Maitlis, P. M. *Can. J. Chem.* **1968**, *46*, 3879. (c) McClure, G. L.; Baddley, W. H. *J. Organomet. Chem.* **1970**, *25*, 261.

(14) Furlani, A.; Collamati, I.; Sartori, G. *J. Organomet. Chem.* **1969**, *17*, 463.

(15) For a reference to cleavage of $\equiv\text{CSi}$ bonds by Pt, see: Ciriano, M.; Howard, J. A. K.; Spencer, J. L.; Stone, F. G. A.; Wade, H. J. *Chem. Soc., Dalton Trans.* **1979**, 1749.

(Bpin)SiMe₃ (**11h**) and the novel tris(boronate ester) Me₃Si(Bpin)C=C(Bpin)₂ (**20**), the latter arising from the diboration of **19**. Apparently, following ≡C–Si oxidative addition to the metal center, a metathetical reaction with B₂(pin)₂ occurs, leading to Si–B and ≡C–B products. This is likely related to the stoichiometric metallacyclopentane–B₂(cat)₂ reaction of Smith^{7a} mentioned earlier. Similar behavior is apparent in reactions involving **1a**. The compound Me₃SiBcat (**21**) was observed as a significant product by GC/MS; however, the ¹H NMR spectrum indicated the presence of several additional products, presumably due to the metathetical reactions described. The isolation of the individual reaction components is still being examined. It has also been reported that reactions between **3a** and Me₃SnSnMe₃ or [(PPh₃)₂Pt(SnMe₃)₂] and **1a** both proceed irreversibly to Me₃SnBcat.^{7b} These results give further evidence for the presence of metathetical reactions involving **1a** and **1c** and are consistent with the observation of products derived from the ≡C–Si bond cleavage in **8h** by the Pt catalyst.

Suzuki, Miyaura, *et al.* reported³ that polar solvents, especially DMF, accelerated the alkyne diboration reaction using B₂(pin)₂ and Pt(PPh₃)₄. Thus, we examined the effect of solvent binding to **1a,c** and **10e** in CDCl₃ with various concentrations of DMF using ¹¹B NMR. The addition of 2 molar equiv of DMF with respect to **10e** resulted in an upfield shift in the resonance from 31.8 to 23.2 ppm, indicative of significant binding to Bcat groups in (*Z*)-PhC(Bcat)=C(Bcat)-Ph. Only a slight shift in the resonance was observed for **1a** in the presence of 2 molar equiv of DMF; however, the addition of 50 molar equiv of DMF resulted in a shift of *ca.* 6 ppm. In contrast, the addition of up to 50 molar equiv of DMF to a solution of **1c** resulted in no significant shift in the ¹¹B NMR resonance. This is consistent with the greater Lewis acidity of Bcat compounds compared with their Bpin analogues¹⁶ and of the vinyl–bis(boronate esters) compared with the diboron reagents. The reported influence of DMF on reaction rates remains unexplained.

Qualitative Kinetic Examination. A series of *in situ* ¹H NMR experiments were conducted at 52 °C in CDCl₃ solution using 0.113 mmol of alkyne, 0.130 mmol of diboron reagent, and 5–6 mol % of catalyst. Reaction of **1a** with **8a** in the presence of either **3b** or **4** proceeded to *ca.* 50% conversion within 30 min and was complete within *ca.* 4 h. The same reaction using **1c** reached only 50% conversion after 5 h. The relative rates for the three diboron reagents were found to be **1a** > **1c** > **1b**. Thus, our premise that **1a** would be more efficient than **1c** was also verified. The reason for the low activity of **1b** is not clear at this time. Furthermore, addition of 2 equiv of PPh₃ to **4** greatly decreased the rate of the catalyzed diborations, consistent with our postulate that the active catalyst was unlikely to possess more than two bound phosphine ligands. In fact, it would appear that PPh₃ dissociation from the bis(phosphine) catalyst precursors is critical. The progress of the above reactions was determined from a comparison of the integrated areas of resonances attributed to the C≡CCH₂ and C=CCH₂ moieties. Initially, plots of ln[alkyne] vs time were linear, indicating overall first-order kinetics; however, in the latter stages of the reactions, curvature

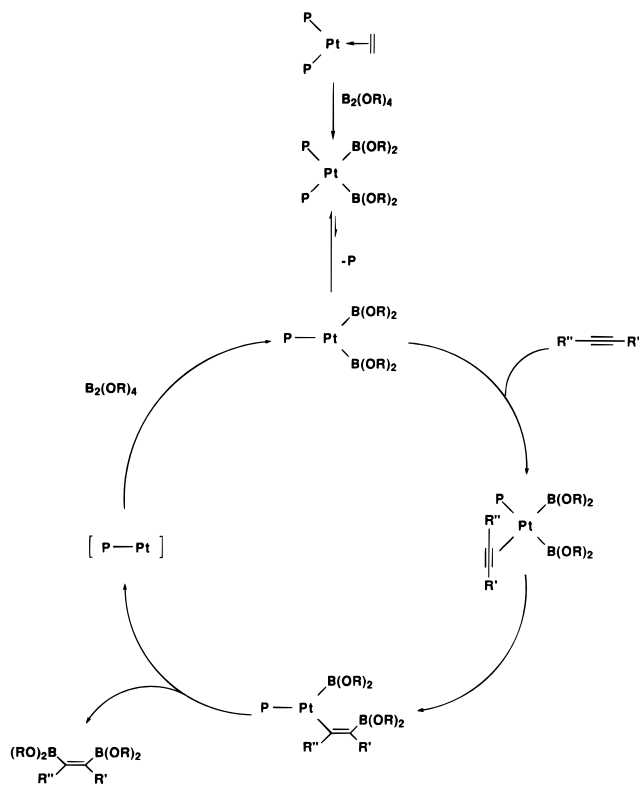
was apparent which is attributed to the partial decomposition of the catalyst in CDCl₃ as described below. Given the fact that the initial concentrations of alkyne and diboron were equal and that they are disappearing at the same rate, the observed first-order disappearance of alkyne implies that the reaction is actually first order in the product of alkyne and diboron concentration, i.e. [alkyne]ⁿ[diboron]^m, where *n* + *m* = 1. Recently, Iverson and Smith^{7b} have performed detailed kinetic studies of both stoichiometric and catalytic variants of the reaction with B₂(cat)₂ (**1a**) using 4-octyne. Under catalytic conditions, in the presence of added PPh₃, the authors observed a first-order dependence on [alkyne], a zero-order dependence on [diboron], and an inverse first-order dependence on [PPh₃], which is consistent with the behavior found in our study.

In a separate series of experiments, under similar reaction conditions (CDCl₃, 52 °C), however, the addition of 4 molar equiv of **1a** also reduced the rate of the reaction significantly. The reason for this is unclear; however, the possibility that an alternative mechanistic pathway involving decomposition of **3a** or **1a** or reversible oxidative addition of **1a** to **3a** seemed reasonable. To test the latter hypothesis, a sample containing equimolar amounts of **3b** and **1a** was heated in toluene for 3 h. The solvent was then removed *in vacuo*, and the crude residue was dissolved in CDCl₃ and analyzed by multinuclear NMR. The proximity and broad character of the resonances in the ³¹P and ¹¹B NMR spectra do not allow a differentiation between **3a** and **3b**, as the resonances are overlapped. The ¹H NMR spectrum, however, in the region of the *tert*-butyl groups, displayed resonances due to the presence of free **1b** (δ_H 1.36 ppm), as well as that for **3b** (δ_H 1.20 ppm), indicating the presence of an equilibrium between **3a** and **3b** which favors the production of **3a** to a very slight degree. No additional resonances were present to suggest the formation of either mixed B–B compounds or Pt–bis(boryl) compounds containing two different types of boryl ligands. Thus, the most likely process for the exchange of the boryl ligands (at least under these conditions) involves B–B reductive elimination and then B–B oxidative addition (Pt(II) → Pt(0) → Pt(II)) rather than B–B oxidative addition and then B–B reductive elimination (Pt(II) → Pt(IV) → Pt(II)), as the latter might be expected to lead to boryl group scrambling.

Mechanistic Details. In reactions involving **5a,b** no catalytic activity for the addition of **1a** to **8a** at 52 °C in CDCl₃ was observed. Similar behavior was apparent in the reaction involving the internal alkyne **8g**, in toluene at 80 °C using **5a**, which showed no activity over 66 h. Interestingly, under the same conditions (i.e. toluene, 80 °C), the reaction proceeded to greater than 90% completion after a period of 2 weeks when **5b** was employed as the catalyst precursor. Clearly, a *trans*-(PPh₃)₂Pt(Bcat)₂ isomer is not the catalytically active species in these reactions, and it seems highly likely that phosphine dissociation even from the bis(phosphine) complexes is required. This result provides additional insight into the mechanism of these catalytic reactions first proposed by Miyaura and Suzuki and co-workers.^{3a} While the present work was in progress, Iverson and Smith reported^{7a} that **3a** reacts stoichiometrically with 4-octyne in the presence of 1.5 mol equiv of **1a** to give the 1,2-vinyl–bis(boronate ester) diboration product and **3a**. These authors also

(16) Nguyen, P.; Dai, C.; Taylor, N. J.; Power, W. P.; Marder, T. B.; Pickett, N. L.; Norman, N. C. *Inorg. Chem.* **1995**, *34*, 4290.

Scheme 7



reported that the alkyne complex $[(\text{PPh}_3)_2\text{Pt}(\eta^2\text{-4-ocytine})]$ reacted with **1a** to generate **3a** with loss of alkyne, indicating that the initial step in the mechanism of these reactions involves the oxidative addition of B–B rather than the coordination of alkyne to the metal.

Scheme 7 illustrates a more detailed description of the proposed mechanism involved in the catalytic diboration of alkynes. The first step is rapid and involves the formation of the oxidative-addition product (**3**). This can be accomplished by reaction of **1a** or **1c** with **4** or, alternatively, with **3b** as discussed above. The fact that **3b** was more stable than **3a** in initial attempts to isolate the oxidative addition products led to its initial choice as a catalyst precursor; however, isolated samples of **3a** have been examined and were found to exhibit similar catalytic activity. The next step in the catalytic cycle should involve the dissociation of a phosphine ligand and association of the alkyne, as it has been shown that the addition of PPh_3 or the presence of a more strongly bound bidentate phosphine inhibits the reaction. This intermediate has not been detected, although ^1H NMR studies in CDCl_3 do indicate the presence of resonances attributable to *cis*- $[(\text{PPh}_3)_2\text{Pt}(\text{B}(\text{OR}))_2]$ throughout the course of the reaction. This may be an indication that the bis(phosphine) bis(boryl) complex is the catalyst resting state and that alkyne binding or alkyne insertion into the metal–boryl bond may be rate-determining (*vide infra*). The reductive elimination of the diborated olefin product is probably rapid and completes the catalytic cycle. The role of phosphine in the latter stages of the catalytic cycle is unknown. Either the phosphine can add to the metal center upon reductive elimination of the product or the mono(phosphine) complex may add another 1 equiv of diboron reagent and continue the catalytic cycle. As we do not observe free PPh_3 in NMR spectra of solutions of **3a–c**, and the broad nature of the ^{31}P NMR resonances can be attributed to coupling with ^{11}B , it would appear that the

equilibrium between compounds **3a–c** and a mono-(phosphine) species lies well on the side of the bis-(phosphine) complexes.

In the presence of PPh_3 , Iverson and Smith reported^{7b} that **3a** shows no reaction, while **3c** exists in an equilibrium with $\text{Pt}(\text{PPh}_3)_4$ (**2**) and $\text{B}_2(\text{pin})_2$. Alternatively, the reaction of **3c** with $\text{B}_2(\text{cat})_2$ proceeds irreversibly to **3a** and $\text{B}_2(\text{pin})_2$. This reversibility of the B–B bond activation which was observed could contribute to the reduced rates associated with catalytic reactions involving $\text{B}_2(\text{pin})_2$ reported in this work and elsewhere.³ In addition, this presumably accounts for the requirement that a large excess of $\text{B}_2(\text{pin})_2$ be present for the isolation of **3c** when it is synthesized from $\text{Pt}(\text{PPh}_3)_4$ (**2**).³

Catalytic Addition of B–B Bonds to 1,3-Diynes.

The addition of 2 equiv of $\text{B}_2(\text{cat})_2$ (**1a**) to 4-MeO- $\text{C}_6\text{H}_4\text{C}\equiv\text{CC}\equiv\text{CC}_6\text{H}_4\text{-4-OMe}$ (**9a**) proceeded smoothly to give the novel tetrakis(boronate ester) compound (*Z,Z*)-(4-MeOC₆H₄)C(Bcat)=C(Bcat)C(Bcat)=C(4-MeOC₆H₄)-(Bcat) (**14a**) within 3 h using catalyst precursor **3b** or **4** (Scheme 4). Again, the addition of PPh_3 to the reaction catalyzed by **4** greatly reduced the rate of the reaction. Attempts to isolate the intermediate (*Z*)-(4-MeOC₆H₄)C(Bcat)=C(Bcat)C≡C-(4-MeOC₆H₄) (**12a**) using 1 equiv of **1a** were unsuccessful, as mixtures of **12a**, **14a**, and unreacted diyne **9a** were observed, indicating that the second addition of diboron occurs at a rate similar to the first addition of diboron reagent. The reaction of **1a** with $\text{Me}_3\text{SiC}\equiv\text{CC}\equiv\text{CSiMe}_3$ (**9b**), on the other hand, was very slow. Examination of GC/MS data revealed that the diyne was still present even after *ca.* 40 h. We were unable to detect the presence of the intermediate compound $\text{Me}_3\text{SiC}\equiv\text{CC}(\text{Bcat})=\text{C}(\text{Bcat})\text{SiMe}_3$ (**12b**) by GC/MS, and thus, the extent of the reaction could not be determined. As a result, the toluene reaction mixture was layered with hexanes and cooled to -36°C , resulting in the formation of a white precipitate. The ^1H and ^{13}C NMR spectra of this product, however, were complex, indicating a variety of products which could not be characterized unambiguously.

Addition of the first equivalent of $\text{B}_2(\text{pin})_2$ (**1c**) to diyne **9a** was rapid to give (*Z*)-(4-MeOC₆H₄)C(Bpin)=C-(Bpin)C≡C-(4-MeOC₆H₄) (**13a**), whereas addition of the second equivalent of **1c** to produce (*Z,Z*)-(4-MeOC₆H₄)C-(Bpin)=C(Bpin)C(Bpin)=C(4-MeOC₆H₄)-(Bpin) (**15a**) was sluggish. This allowed for the preparation and characterization of the intermediate species **13a** from the reaction of **9a** with 1 equiv of **1c** (Scheme 4). The unsymmetrical nature of the product formed gives rise to two resonances for the chemically inequivalent methoxy groups, as expected, in the ^1H (3.80, 3.75 ppm) and ^{13}C (55.1, 55.0 ppm) NMR spectra. In the preparation of **15a**, GC/MS analysis indicated that small amounts of diyne **9a** remained after 3 h; therefore, the reaction mixture was left for 16 h to ensure completion. The symmetric tetrakis(boronate ester) product displays a resonance for only one chemically distinct methoxy group (δ_{H} 3.73 ppm; δ_{C} 55.1); however, there are four distinct resonances for the CH_3 groups of the Bpin moieties in the ^1H and ^{13}C NMR spectra. Initial molecular mechanics calculations on a model for **15a** indicate that hindered or geared rotation of the Bpin groups occurs, giving rise to four separate signals in this region of the ^1H NMR spectrum (1.29, 1.24, 1.00, 0.94

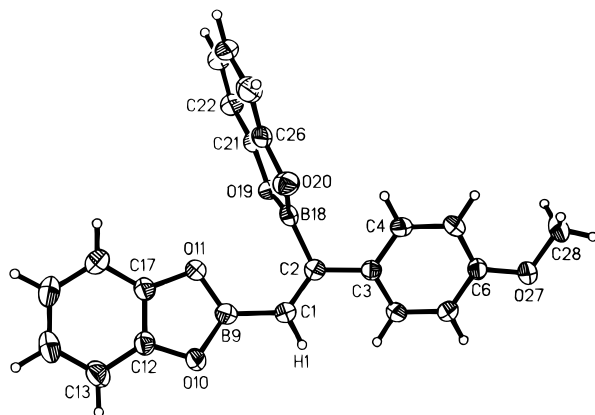


Figure 5. Molecular structure of *(E)*-(4-MeO-C₆H₄)C(B(1,2-O₂C₆H₄))=CH(B(1,2-O₂C₆H₄)) (**10c**), with 50% probability ellipsoids.

ppm). This is also apparent in the ¹³C NMR spectrum, in which there are two quaternary carbons present (83.0, 82.9 ppm) and four resonances in the region for primary carbon atoms associated with the CH₃ groups of the Bpin moiety (25.2, 24.8, 24.5, 24.3 ppm). Thus, the (Bpin)₄ compounds are quite sterically encumbered.

The reaction involving bis(trimethylsilyl)butadiyne (**9b**) and **1c** was very slow, consistent with results from the reaction involving **1a**. Monitoring the reaction by GC/MS indicated that the reaction proceeded to form the intermediate bis(boronate ester) (*Z*)-Me₃SiC(Bpin)=C(Bpin)C≡CSiMe₃ (**13b**) prior to the subsequent reaction to produce the tetrakis(boronate ester) (*Z,Z*)-Me₃SiC(Bpin)=C(Bpin)C(Bpin)=C(Bpin)SiMe₃ (**15b**). This latter step required a reaction time of 77 h to reach completion. The extent of the reaction in this case could be determined by GC/MS by monitoring the disappearance of compounds **13b** and **1c**. As with the preparation of **14b**, NMR data could not be assigned due to the presence of products derived from the C≡CSiMe₃ metathetical reactions described above. The preparation of **13b** involving only 1 equiv of **1c** required a reaction time of 6 h to reach completion, and the absence of metathetical reactions allowed for complete NMR characterization. The mass of the parent ion M⁺ for the tetrakis(boronate esters) **14a,b** and **15a,b** exceeds the mass range of the GC/MS (650 amu) used in these investigations; however, compounds **15a,b** have been identified (M + H⁺) by directly introducing samples into the electrospray unit of an HPLC/MS/MS spectrometer, as described in the Experimental Section. Interestingly, peaks attributable to (**15b** + *n*H₂O + H⁺) (*n* = 0–4) were observed (aqueous CH₃CN was employed in the analysis), indicating that **15b** is stable to H₂O and is also capable of binding up to four molecules of water.

Molecular Structures of Organoboronate Esters. The structure of *(E)*-(4-MeO-C₆H₄)C(Bcat)=CH(Bcat) (**10c**; Figure 5) represents the first structural evidence of the *cis* disposition of the boron substituents in the products derived from the catalytic diboration of a terminal alkyne. The C=C bond distance (1.348(2) Å) is typical for olefin compounds and is similar to or shorter than the respective C=C bond distances in the internal alkene and diene derivatives (**10e** (two crystallographically independent molecules in the unit cell), 1.353(2) and 1.358(2); **10f**, 1.357(2); **11g**, 1.358(2); **14a**, 1.373(3) and 1.362(2) Å). Replacement of the methoxy functionality with a cyano group results in no significant changes in the C=C distance (**10d**, 1.349(2) Å). The

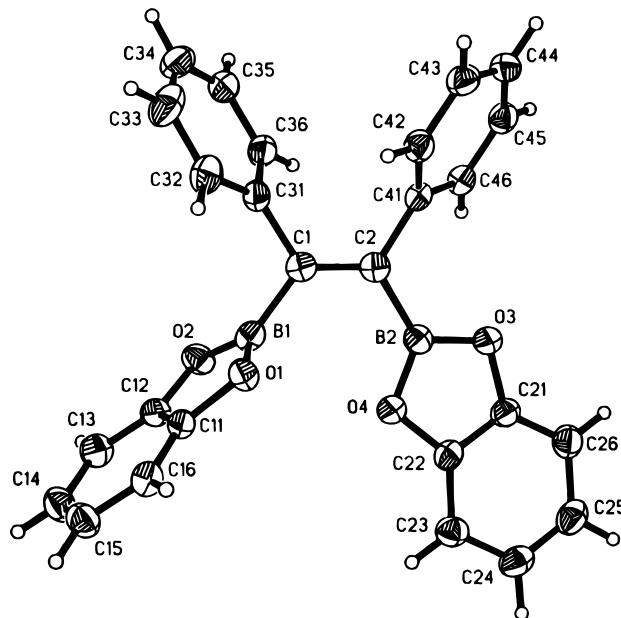


Figure 6. Molecular structure of *(Z)*-(C₆H₅)C(B(1,2-O₂C₆H₄))=C(C₆H₅)C(B(1,2-O₂C₆H₄)) (**10e**), with 50% probability ellipsoids. One of the two similar but independent molecules is shown.

C(1)–B(9) bond distance (1.526(2) Å) is also smaller when compared to the C(2)–B(18) bond distance (1.566(2) Å) and those in the other Bcat derivatives described (**10d**, 1.569(2), 1.535(2); **10e**, 1.559(2), 1.551(2), 1.553(2), 1.562(2); **10f**, 1.565(2), 1.553(2); **14a**, 1.541(3), 1.570(3), 1.565(3), 1.546(3) Å). Both deviations are presumably due to the decrease of steric repulsion present at the terminal carbon atom. The B–C bond distances for **11g** (1.580(2) and 1.564(2) Å) are slightly larger due to the steric constraints of the Bpin functional group. The structures of **10d,f** and **11g** are similar to that of **10e** and will not be discussed in detail in this report.¹²

Relief of steric congestion at the terminal carbon atom in **10c** is also apparent in the bond angles, with the angle formed by B(9)–C(1)–C(2) (124.4(1)°) being larger than any of the other sp²-hybridized bond angles (C(1)–C(2)–C(3), 123.6(1)°; C(1)–C(2)–B(18), 120.1(1)°; B(18)–C(2)–C(3), 116.3(1)°) in the structure. The decrease in the B(18)–C(2)–C(3) angle also indicates that the boryl moieties on adjacent carbon atoms of the olefin have a slightly larger influence than the aryl counterparts in determining the steric requirements in the solid-state structure of this compound and that this depends upon the C=C(boryl) rotational conformation. The interplanar angle between the mean plane formed by the aryl carbons, C(3)–C(8), and the mean plane formed by B(9), C(1), C(2), C(3), B(18) is 16.9°, and the planes formed by the boryl ligands subtend interplanar angles of 7.0 and 83.9° (B(9), O(10), O(11), C(12)–C(17) and B(18), O(19), O(20), C(21)–C(26), respectively) with respect to the C₃B₂ alkene plane. This results in the aryl group and one Bcat ligand being almost coplanar with the alkene mean plane while the other Bcat ligand is almost perpendicular due to steric constraints.

The structure of *(Z)*-(C₆H₅)C(Bcat)=C(Bcat)(C₆H₅) (**10e**; Figure 6) represents the first structural evidence of the *cis* disposition of the boron substituents in the products derived from the catalytic diboration of an internal alkyne. In this structure, the C=C and B–C bond lengths in the two crystallographically independent molecules correlate well, although there are sig-

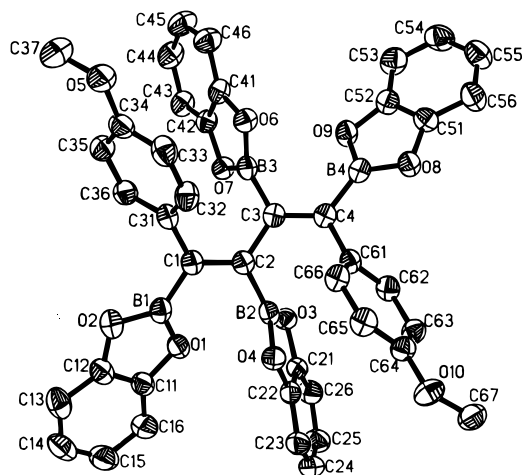


Figure 7. Molecular structure of (Z,Z) -(4-MeO-C₆H₄)C(B(1,2-O₂C₆H₄))=C(B(1,2-O₂C₆H₄))C(B(1,2-O₂C₆H₄))=C(4-Me-OC₆H₄)(B(1,2-O₂C₆H₄)) (**14a**), with 50% probability ellipsoids.

nificant differences in some of the bond angles. In molecule 1, the C(31)–C(1)–B(1) and C(41)–C(2)–B(2) angles are reduced from 120 to 111.84(12)° and 116.91(13)°, respectively, whereas the angles formed by B(1)–C(1)–C(2) (126.51(14)°) and C(31)–C(1)–C(2) (121.64(13)°) are greater than 120°. In molecule 2, the bond angles around C(51), namely, B(3)–C(51)–C(81) = 119.29(13)°, B(3)–C(51)–C(52) = 119.28(14)°, and C(81)–C(51)–C(52) = 121.43(14)°, indicate that the steric requirements in the solid state may be relieved by changes in the interplanar angles of the boryl and aryl functional groups, as values are approaching that expected for pure sp² hybridization. Clearly, some balance must exist between the steric effects of the groups on adjacent olefinic carbon atoms and the interplanar angles formed by these groups. This is also evident in the bond angles formed in the other half of molecule 2, which are closer to typical values found in molecule 1 (B(4)–C(52)–C(91) = 111.03(12)°; B(4)–C(52)–C(51) = 125.23(14)°; C(91)–C(52)–C(51) = 123.58(14)°). Interplanar angles of 76.3° (B(1), O(1), O(2), C(11)–C(16)), 10.9° (B(1), O(1), O(2), C(11)–C(16)), 55.9° (C(31)–C(36)), and 57.7° (C(41)–C(46)) are formed with respect to the mean plane defined by C(1), C(2), B(1), B(2), C(31), and C(41) in molecule 1. In molecule 2, the boryl groups form interplanar angles of 4.6° (B(3), O(5), O(6), C(61)–C(66)) and 77.5° (B(4), O(7), O(8), C(71)–C(76)) while the aryl groups form angles of 56.7° (C(81)–C(86)) and 54.3° (C(91)–C(96)) with respect to the mean plane defined by C(51), C(52), B(3), B(4), C(81), C(91).

The structure of (Z,Z) -(4-MeOC₆H₄)C(Bcat)=C(Bcat)–C(Bcat)=C(4-MeOC₆H₄)(Bcat) (**14a**; Figure 7) is the first determined for a butadiene tetrakis(boronate ester) and demonstrates the *cis* disposition of the boron substituents in the products derived from the catalytic tetraboration of an internal diyne. This compound crystallizes in the *s-trans* conformation with a torsion angle of 150.7° with respect to C(1), C(2), C(3), and C(4), but the bond angles displayed in the structure deviate only slightly from 120°. The interplanar angles formed with respect to the mean plane defined by C(1), C(2), B(1), B(2), C(31), and C(3) are 18.6° (B(1), O(1), O(2), C(11)–C(16)), 66.5° (B(2), O(3), O(4), C(21)–C(26)), and 58.4° (C(31)–C(36)) and the mean planes formed by (B(3), O(6), O(7), C(41)–C(46)), (B(4), O(8), O(9), C(51)–C(56)),

and (C(61)–C(66)) display very similar interplanar angles of 57.6, 18.3, and 66.1°, respectively, in relation to the mean plane defined by C(3), C(4), B(3), B(4), C(2), and C(61). Thus, boryl ligands in the 1- and 4-positions are nearly coplanar with their C=C unit, whereas boryl ligands in the 2- and 3-positions are closer to a perpendicular orientation, as are the aryl rings.

Decomposition of Catalysts. The completion of the catalytic reactions in toluene (80 °C) was accompanied by a noticeable change in color of the solutions, usually to a deep red color associated with the decomposition of the catalyst. When slight excesses of B₂(cat)₂ or B₂(pin)₂ were used, very minute resonances due to the presence of B₂(cat)₃ (**6**)¹⁷ or B₂(pin)₃ (**7**)¹⁸ were also detected in the ¹H, ¹¹B, and ¹³C NMR spectra of the crude reaction mixtures. In addition, relatively large amounts of **6** or **7** could be observed in the spectra of reactions requiring extended reaction times, such as those involving π-acceptor-substituted alkynes, in which additional diboron reagent was required to complete the catalytic reaction. As well, the *in situ* spectra recorded during the formation of **3c** also exhibited resonances in the ¹¹B{¹H} NMR spectrum consistent with the formation of B₂(pin)₃ (**7**). It seemed unlikely that the initially reported value for **3c** (δ_B 21.50 ppm)^{3a} was due to the presence of an oxidative-addition product as originally proposed, but rather, we believe that this sharp resonance corresponds to the byproduct **7**. Recent reports by the same authors^{3b} have provided a new value (δ_B 46.3 ppm) for **3c** which is consistent with those obtained for similar compounds described in this work. Recently, related research in our laboratory has resulted in the isolation of authentic **7** (δ_B 21.7 ppm)¹⁸ confirming (by single-crystal X-ray diffraction) the nature of this compound. In addition, **7** is formed in the reaction of 2 equiv of BH₃ with 3 equiv of pinacol (albeit in low yield) and has also been identified as a common byproduct in the synthesis of **1c**. In the latter case, recrystallization from hexanes resulted in pure samples of **1c**. It seemed apparent, therefore, that the subsequent decomposition of catalyst was intimately related to the formation of **6** or **7**. A series of *in situ* NMR experiments were performed to investigate the stability of the catalysts, the effect of solvent on the decomposition, and the reaction between B₂(cat)₃ (**6**) and (PPh₃)₂Pt(η-C₂H₄) (**4**).

In the absence of excess B₂(cat)₂ (**1a**) or alkyne, solutions of **3a** in CDCl₃ began to decompose within 1 h. After 1 week, new resonances were apparent in the ¹H, ¹¹B{¹H}, and ³¹P{¹H} NMR spectra. The ³¹P{¹H} NMR spectrum indicated the presence of two major compounds with the same (within experimental error) chemical shifts but with differing J_{Pt–P} coupling constants (δ_P 28.7 ppm; J_{Pt–P} = 1634 and 3021 Hz). The hydride region of the ¹H NMR spectrum exhibited a triplet at –16.3 ppm (J_{P–H} = 13 Hz, J_{Pt–H} = 1197 Hz). The remaining portion of the ¹H NMR spectrum displayed several overlapping resonances in the aromatic region consistent with PPh₃- and Bcat-containing compounds. These results are consistent with the presence of **3a** and the formation of *trans*-(PPh₃)₂Pt(H)(Cl), which has been characterized previously.^{19a–c} The nature of this compound has been determined unambiguously by means of X-ray crystallography.^{19d,e} The ¹¹B{¹H} NMR

(17) Westcott, S. A.; Blom, H. P.; Marder, T. B.; Baker, R. T.; Calabrese, J. C. *Inorg. Chem.* **1993**, *32*, 2175.

(18) Clegg, W.; Scott, A. J.; Dai, C.; Lesley, G.; Marder, T. B.; Norman, N. C.; Farrugia, L. J. *Acta Crystallogr.*, in press.

spectrum exhibited only one new resonance at 23.7 ppm, which is consistent with the formation of $B_2(\text{cat})_3$ (**6**) in CDCl_3 .¹⁷

In contrast, C_6D_6 solutions of **3a** are stable for long periods of time at room temperature. After 4 weeks, the $^{31}\text{P}\{^1\text{H}\}$ NMR spectrum indicated the presence of **3a** (δ_{P} 29.8 ppm; $J_{\text{Pt-P}} = 1622$ Hz) and a new resonance at 24.2 ppm ($J_{\text{Pt-P}} = 2900$ Hz). The nature of this new product is not known; however, the $^{11}\text{B}\{^1\text{H}\}$ NMR spectra did indicate that significant quantities of $B_2(\text{cat})_3$ (**6**) were present (δ_{B} 22.4 ppm in C_6D_6). Solutions of **3a** in $\text{C}_6\text{D}_6/\text{THF}$ were observed to decompose more rapidly compared to those in CDCl_3 or C_6D_6 . Although the reason for this is uncertain, the use of THF as a solvent for the catalytic reactions was avoided.

The results in CDCl_3 indicated that a reaction was occurring between the Pt center and the solvent, as this was the only source of Cl available. To determine the role of the boryl groups in this decomposition, we examined the *in situ* decomposition of $(\text{PPh}_3)_2\text{Pt}(\eta\text{-C}_2\text{H}_4)$ (**4**) in both CDCl_3 and C_6D_6 , as this would give an indication of which products could be forming from interactions involving the $(\text{PPh}_3)_2\text{Pt}$ fragment and solvent.

The *in situ* $^{31}\text{P}\{^1\text{H}\}$ NMR spectrum of a C_6D_6 solution of **4** (δ_{P} 34.9 ppm; $J_{\text{Pt-P}} = 3741$ Hz) indicated no noticeable changes over a period of 2 h. A CDCl_3 solution of the same sample of **4**, however, exhibited resonances attributable to at least two different Pt-Cl-containing compounds. The behavior in solution of **4** and related Pt(0) compounds such as $(\text{PPh}_3)_3\text{Pt}$ and $(\text{PPh}_3)_2\text{Pt}$ have been studied extensively.^{20–22} Malatesta and Cariello reported^{20a} that samples of $(\text{PPh}_3)_3\text{Pt}$ undergo dissociation in solution and first proposed the formation of a $(\text{PPh}_3)_2\text{Pt}$ species to account for the behavior observed. Ugo *et al.* reported^{20b} the synthesis of $(\text{PPh}_3)_2\text{Pt}$ by several routes and subsequently proposed the formation of a trimeric cluster^{20c} to account for the red compounds formed upon heating of the $(\text{PPh}_3)_2\text{Pt}$ sample. Glockling and co-workers,²¹ upon studying reactions of **4**, reformulated this trimeric cluster and related decomposition products as arising from *ortho*-metalation reactions involving the phosphine ligands. Subsequent to this report, Carty *et al.*^{22a} reported structural evidence of facile P–C bond cleavage²³ giving rise to phosphido-bridged Pt clusters which arise by refluxing solutions of $(\text{PPh}_3)_4\text{Pt}$ (**2**). In this study, $^{31}\text{P}\{^1\text{H}\}$ NMR analysis of the yellow solution formed initially indicated the presence of **4** (δ_{P} 34.4 ppm; $J_{\text{Pt-P}} = 3718$ Hz), *trans*- $(\text{PPh}_3)_2\text{Pt}(\text{H})(\text{Cl})$ (δ_{P} 28.7 ppm),

and *cis*- $(\text{PPh}_3)_2\text{PtCl}_2$ (δ_{P} 14.7 ppm; $J_{\text{Pt-P}} = 3675$ Hz)²⁴ and new resonances at 26.5 ppm (s, $J_{\text{Pt-P}} = 3187$ Hz), 19.7 ppm (d, $J = 17$ Hz), and 17.6 ppm (d, $J = 17$ Hz). The resonance at 26.5 ppm was the most abundant of the new resonances formed and is attributed to the formation of solvated $(\text{PPh}_3)_2\text{Pt}$ from ethylene dissociation.^{20d} The ^1H NMR spectrum also exhibited a resonance due to free ethylene at 5.2 ppm. Previous reports for the isolation of the compound $(\text{PPh}_3)_2\text{Pt}$ indicated^{20b} that the compound was yellow, which is consistent with the change in color of the solution noted in this work. It is unfortunate that no ^{31}P chemical shifts were reported by the authors to enable a comparison on this basis. The pair of doublets observed could be due to *cis*- $(\text{PPh}_3)_2\text{Pt}(\text{H})(\text{CCl}_3)$, which would be consistent with the observed multiplicity of the resonances and reaction with solvent. This compound is very unstable in solution and disappears over time. Minute resonances in the form of four broad multiplets were also present in the hydride region of the ^1H NMR spectrum (*ca.* –3 to –5 ppm) which are consistent with the formation of an additional hydrido–platinum compound. The possibility of the formation of *cis*- $(\text{PPh}_3)_2\text{Pt}(\text{H})(\text{Cl})$ seemed unlikely, since the *trans* isomer has been shown to be the only isomer present in solution.²⁵

As mentioned above, the formation of $B_2(\text{cat})_3$ (**6**) and $B_2(\text{pin})_3$ (**7**) in catalytic reactions (toluene, 80 °C) involving π -acceptor-substituted alkynes such as **8d** indicated that alternative reactions involving the diboron reagent and/or catalyst may be occurring in solution. We decided, therefore, to examine the reaction between **6** and **4**. These reactions were followed by *in situ* NMR spectroscopy in CDCl_3 and C_6D_6 .

In CDCl_3 , the $^{31}\text{P}\{^1\text{H}\}$ NMR spectrum indicated the formation of a large quantity of *trans*- $(\text{PPh}_3)_2\text{Pt}(\text{H})(\text{Cl})$ when compared to the decomposition of **4** alone. The addition of **6** to the solution clearly enhanced the formation of this hydrido–platinum compound. In addition, the formation of resonances assigned above as $(\text{PPh}_3)_2\text{Pt}$ and *cis*- $(\text{PPh}_3)_2\text{PtCl}_2$ were also apparent. Two additional resonances (δ_{P} 23.6 and 29.9 ppm) which were not present in the decomposition of **4** or **3a** did appear. The resonance at 23.6 ppm ($J_{\text{Pt-P}} = 2870$ Hz) has been assigned to the compound *trans*- $(\text{PPh}_3)_2\text{Pt}(\text{Cl})(\text{Bcat})$.²⁶ The nature of the compound corresponding to the resonance at 29.9 ppm is not certain; however, the solution was observed to turn dark red. Solutions of **4** in CDCl_3 were initially yellow and became red only after extended periods of time. The compound *trans*- $(\text{PPh}_3)_2\text{Pt}(\text{Cl})(\text{Bcat})$ is a colorless compound when pure; therefore, the red color observed may correspond to the compound giving rise to this new, unassigned resonance. As mentioned, the formation of *ortho*-metalation products or polymetallic complexes derived from facile P–C bond cleavage giving rise to bridging phosphido clusters has been proposed to account for the products obtained as red solutions. The ^{31}P spectra of these compounds, however, are expected to be more complex due to the presence of the inequivalent phosphine ligands which would be formed by either process. No resonances due

(19) (a) Chatt, J.; Shaw, B. L. *J. Chem. Soc.* **1962**, 5075. (b) Ugo, R.; LaMonica, G.; Cariati, F.; Cenini, S.; Conti, F. *Inorg. Chim. Acta* **1970**, *4*, 390. (c) McFarlane, W. *J. Chem. Soc., Dalton Trans.* **1974**, 324. (d) Bender, R.; Braunstein, P.; Jud, J.-M.; Dusausoy, Y. *Inorg. Chem.* **1984**, *23*, 4489. (e) Lesley, G.; Marder, T. B.; Scott, A. J.; Clegg, W.; Norman, N. C., unpublished results.

(20) (a) Malatesta, L.; Cariello, C. *J. Chem. Soc.* **1958**, 2323. (b) Ugo, R.; Cariati, F.; LaMonica, G. *Chem. Commun.* **1966**, 868. (c) Gillard, R. D.; Ugo, R.; Cariati, F.; Cenini, S.; Bonati, F. *Chem. Commun.* **1966**, 869. (d) Cook, C. D.; Jauhal, G. S. *Can. J. Chem.* **1967**, *45*, 301.

(21) Glockling, F.; McBride, T.; Pollock, R. J. *J. Chem. Soc., Chem. Commun.* **1973**, 650. For related reactions involving Ir see: Bennett, M. A.; Milner, D. L. *J. Am. Chem. Soc.* **1969**, *91*, 6983.

(22) (a) Taylor, N. J.; Cheih, P. C.; Carty, A. J. *J. Chem. Soc., Chem. Commun.* **1975**, 448. (b) In further work by this group, the $^{31}\text{P}\{^1\text{H}\}$ NMR spectrum (toluene-*d*₈) of $(\text{PPh}_3)_2\text{Pt}_2(\mu\text{-PPh}_2)_2$, which was the major decomposition product observed by a variety of synthetic routes, was reported: δ 163.3 ppm (a series of triplets, PPh₂), 28.3 (intense multiplet, PPh₃). Hartstock, F. W. M.Sc. Thesis, University of Waterloo, 1981. This compound was characterized as being only sparingly soluble in common NMR solvents.

(23) (a) Patel, H. A.; Fischer, R. G.; Carty, A. J.; Naik, D. V.; Palenik, G. J. *J. Organomet. Chem.* **1973**, *60*, C49. (b) Cullen, W. R.; Harbourne, D. A.; Liengme, B. V.; Sams, J. R. *Inorg. Chem.* **1970**, *9*, 702.

(24) See for example: Al-Najjar, I. *Inorg. Chim. Acta* **1987**, *128*, 93 and references therein.

(25) Collamati, I.; Furlani, A.; Attioli, G. *J. Chem. Soc. A* **1970**, 1694.

(26) Lesley, G.; Marder, T. B.; Scott, A. J.; Clegg, W.; Norman, N. C., unpublished results.

to bridging phosphido groups were observed.^{22b} The resonance observed in this work (29.9 ppm) would be more consistent with a polymeric cluster involving $(\text{PPh}_3)_2\text{Pt}$ vertices similar to the compounds initially proposed by Ugo *et al.*,^{20c} in which the phosphine ligands are chemically and magnetically equivalent.

In the reaction of **6** with **4** in C_6D_6 , an insoluble red oil formed rapidly, accompanied by the appearance of a new hydride resonance in the ^1H NMR spectrum (t , $\delta_{\text{H}} = 23.2$ ppm; $J_{\text{P-H}} = 13.7$ Hz; $J_{\text{Pt-H}} = 1359$ Hz). The $^{31}\text{P}\{-^1\text{H}\}$ NMR spectrum also exhibited new resonances at 30.6 ppm ($J_{\text{Pt-P}} = 3061$ Hz) and 23.1 ppm (minor product, no Pt satellites were observed) in addition to **4**. The resonance at 30.6 ppm may be the result of the formation of polymetallic compounds as noted above, as a red product was observed to form and the chemical shift is quite similar to the one observed in CDCl_3 at 29.9 ppm (a slight downfield shift is also present in changing solvent from CDCl_3 to C_6D_6 for samples of **4**). The value of the Pt–P coupling constant for the reaction in CDCl_3 could not be determined for comparison. The remaining resonance at 23.1 ppm would, therefore, represent a hydrido–platinum species corresponding to the hydride resonances observed in the ^1H NMR spectrum. The formation of this complex is also enhanced by the addition of **6** when compared to the decomposition of **4** in the absence of **6** in C_6D_6 . The origin and nature of this species are uncertain. The possibility of *ortho*-metalation reactions, similar to those mentioned above, cannot be ruled out. Hartwig *et al.*²⁷ have recently demonstrated the photolytic activation of benzene and toluene by $\text{CpFe}(\text{CO})_2(\text{Bcat})$. However, the observation of a hydride signal in C_6D_6 would preclude the solvent as the source of the hydride in our case. It seemed unlikely that $(\text{PPh}_3)_2\text{Pt}(\text{H})(\text{Bcat})$ could be responsible for the appearance of the new hydride resonance, since preliminary studies²⁶ involving HBcat and **4** indicate the rapid formation of **3a**, accompanied by the evolution of H_2 . The instability of $(\text{PPh}_3)_2\text{PtH}_2$ compounds has been reported,²⁸ and it is unlikely that this compound is stable enough to be attributed to this resonance.

In addition to the solution behavior mentioned above, ^{11}B NMR spectra for the reactions in both solvents exhibited minor resonances consistent with the formation of $[\text{B}(\text{cat})_2]^-$. The formation of this compound may arise due to self-ionization of $\text{B}_2(\text{cat})_3$ (heterolytic B–O bond cleavage) or, alternatively, as a result of reactions involving the metal center and $\text{B}_2(\text{cat})_3$. It seems likely that the unassigned resonances mentioned above could also arise from B–O bond cleavage or ionic reactions involving boron, occurring at the metal center. It is clear that the formation of hydrido–platinum compounds is enhanced by the addition of $\text{B}_2(\text{cat})_3$, and it would appear that the process occurring also involves solvent interactions, at least in CDCl_3 . The exact nature of this process remains undefined and will be investigated in more detail.

Iverson and Smith^{7b} recently reported that $(\text{PPh}_3)_2\text{Pt}(\text{Bpin})_2$ (**3c**) is prone to reductive elimination in the presence of a variety of substrates, including **1a**, and that in the presence of alkyne an equilibrium exists between **3c** and a $(\text{PPh}_3)_2\text{Pt}(\eta\text{-alkyne})$ complex plus B_2 -

(pin)₂. In this regard, the authors indicated that the possibility of an associative pathway involving the reaction of the Pt–alkyne compound with **1c** could not be ruled out. In addition, the same authors noted that kinetic investigation of stoichiometric and catalytic reactions involving **1a** and **3a** were first order in catalyst concentration, under pseudo-first-order conditions in alkyne concentration. The fact that $(\text{PPh}_3)_2\text{Pt}(\text{Bpin})_2$ (**3c**) undergoes reductive elimination indicated that reactions with CDCl_3 may significantly reduce the concentration of the catalyst and, thus, the rate of the reaction when comparing kinetic results from reactions involving **1a** and **1c**. This may contribute to the reduced rates observed in our initial kinetic studies with 1-octyne (**8a**) and $\text{B}_2(\text{pin})_2$ (**1c**), as **4** was employed as the catalyst. As mentioned above, comparisons in this study were drawn from initial portions of plots of $\ln[\text{alkyne}]$ vs time, which were linear for reactions involving **1a** and **1c**. Deviations from linearity at the latter stages of the reactions were apparent in the presence of **1a** or **1c**, and also, when **1c** was used as the diboron reagent, the deviation was more pronounced.

The decomposition noted above does not appear to interfere with the catalysis in toluene at 80 °C with the above-noted exceptions. It is clear that the choice of solvent and purity of the diboron reagents (i.e. absence of any $\text{B}_2(\text{cat})_3$ and $\text{B}_2(\text{pin})_3$ in the synthesis of **1a** and **1c**, respectively) are crucial to accurately determine the kinetic behavior of these systems. It should be noted that the samples of $\text{B}_2(\text{cat})_2$ and $\text{B}_2(\text{pin})_2$ used in this study were rigorously purified and that their purity was checked carefully prior to use.

Conclusions

We have shown that $(\text{PPh}_3)_2\text{Pt}$ complexes, either Pt(II) bis(boryls) or Pt(0)–ethylene complexes, are more efficient catalyst precursors than $[\text{Pt}(\text{PPh}_3)_4]$ for the diboration of alkynes and that $\text{B}_2(\text{cat})_2$ reacts faster than $\text{B}_2(\text{pin})_2$, which in turn is much faster than $\text{B}_2(4\text{-Bu}^t\text{-cat})_2$. Initial results indicate that decomposition of the Pt(II) bis(boryl) compounds gives rise to the boron-containing products $\text{B}_2(\text{cat})_3$ and $\text{B}_2(\text{pin})_3$. The resulting $[(\text{PPh}_3)_2\text{Pt}]$ species may react with solvent in the absence of diboron reagent or alkyne, or with $\text{B}_2(\text{cat})_3$, to produce metal hydride products incapable of catalyzing the desired reactions. Furthermore, the stability of $[(\text{PPh}_3)_n\text{Pt}(\eta\text{-alkyne})]$ compounds and subsequent competing reactions leads to reduced rates for the diboration of π -acceptor-substituted alkynylarene derivatives. An important step in the catalyzed diboration of alkynes appears to be the dissociation of phosphine from the $(\text{PPh}_3)_2\text{Pt}$ complexes, giving rise to a mono-(phosphine)Pt intermediate which serves as the active catalyst in these systems. We have also found that diynes can be either diborated or tetraborated in a controlled fashion using these systems and that novel products, including vinyl-tris(boronate esters), are obtained via $\equiv\text{C-Si}$ bond cleavage with $\text{Me}_3\text{SiC}\equiv\text{CSiMe}_3$. Further work is in progress to develop even more active catalyst precursors involving Pt and Ni mono(phosphine) analogues. Preliminary results employing $(\eta\text{-COD})_2\text{Pt}$ and 1 equiv of $\text{P}(o\text{-tolyl})_3$ demonstrate that this system provides significant activity for addition of $\text{B}_2(\text{pin})_2$ (**1c**) to 4-MeOPhC \equiv CPh-4-OMe (**8g**) at room temperature in toluene.

(27) Waltz, K. M.; He, X.; Muhoro, C.; Hartwig, J. F. *J. Am. Chem. Soc.* **1995**, *117*, 11357.

(28) The inability to isolate dihydride compounds of $(\text{PPh}_3)_2\text{Pt}$ has been noted: Moulton, C. J.; Shaw, B. L. *J. Chem. Soc., Chem. Commun.* **1976**, 365.

Experimental Section

General Considerations. All reactions were performed under a dry nitrogen atmosphere using glovebox techniques. Reaction solvents were dried using the appropriate drying agents and distilled under an N₂ atmosphere: toluene, diethyl ether, and THF from Na/benzophenone, hexanes from Na metal, and DMF from CaH₂. NMR solvents were distilled from CaH₂ (CDCl₃) or Na metal (C₆D₆) following three freeze/pump/thaw cycles. Alkynes were prepared by reported routes²⁹ or obtained from commercial sources. Phenylacetylene and 1-octyne were degassed via three freeze/pump/thaw cycles and vacuum-distilled prior to use. The synthesis of compounds **1a–c** has been discussed previously.^{5,30} All starting reagents were checked for purity using GC/MS and/or NMR prior to use. Melting point determinations were made using a Mel-Temp II (Laboratory Devices) apparatus equipped with a Fluke 51 thermocouple (John Fluke Mfg. Co.) with samples sealed in glass capillary tubes using wax.

Nuclear magnetic resonance experiments were performed on Bruker AC200 or AMX 500 spectrometers at the following frequencies, unless otherwise stated: ¹H, 200 and 500 MHz; ¹³C{¹H}, 50 and 125 MHz; ¹¹B{¹H}, 64 MHz; ³¹P{¹H}, 81 MHz. The ¹H chemical shifts were referenced to the internal standard tetramethylsilane (TMS), and ¹³C chemical shifts were referenced to the solvent resonances as an internal standard. The ¹¹B and ³¹P chemical shifts are referenced to the external standards F₃B·OEt₂ and 85% H₃PO₄, respectively. The ¹¹B NMR spectra were obtained using a background subtraction routine to remove resonances due to borosilicate glass in the NMR probe and NMR tube. This was accomplished by recording the spectrum of an NMR tube containing the same height of pure solvent with collection parameters identical with those for the sample and subtracting this background FID from that of the sample. Spectra were recorded in CDCl₃ unless otherwise stated. Elemental analyses were obtained from M-H-W Laboratories, Phoenix, AZ.

GC/MS analyses were performed on a Hewlett-Packard 5890 Series II/5971A MSD instrument equipped with an HP 7673A autosampler and a fused silica column (30 m × 0.25 mm, cross-linked 5% phenylmethyl silicone). The following operating conditions were used: injector, 260 °C; transfer line, 280 °C; oven temperature was ramped from 70 to 260 °C at the rate of 20 °C/min. UHP grade helium was used as the carrier gas.

The parent ions [M + H]⁺ for compounds **15a,b** were observed by injecting a 10 μL sample of the crude product into a VG/Fisons (Manchester, UK) Quattro II triple quadrupole mass spectrometer fitted with an electrospray source. A 50/50 mixture of H₂O and CH₃CN was used as a carrier solution at a rate of 10 mL/min, and samples were introduced directly into the electrospray source.

Synthesis of *cis*–[(PPh₃)₂Pt(boryl)₂] Compounds. *cis*–[(PPh₃)₂Pt(B(1,2-O₂C₆H₄))₂]·C₇H₈ (3a**).** The compound [(PPh₃)₂Pt(η-C₂H₄)]⁹ (**4**; 1.000 g, 1.337 mmol) was dissolved in toluene (5 mL), and solid B₂(cat)₂ (**1a**; 318 mg, 1.337 mmol) was added portionwise with a spatula. The solution was stirred at ambient temperature, and the evolution of ethylene gas was apparent. A white precipitate began to form immediately, which was collected by filtration after 30 min, washed with cold toluene (5 mL) and dried *in vacuo*: yield 1.236 g (88%); mp 170.2–171.2 °C (dec, 111 °C); ³¹P{¹H} NMR δ 28.7 (br, J_{Pt–P} = 1639 Hz); ¹¹B{¹H} NMR δ 47.0 (br); ¹H NMR δ 7.36 (m, 12H, P(C₆H₅)₃), 7.08 (m, 18H, P(C₆H₅)₃), 6.77 (m, 4H, 1,2-O₂C₆H₄), 6.68 (m, 4H, 1,2-O₂C₆H₄) + toluene of solvation; ¹³C NMR δ 149.7 (s, 4C, ³J_{Pt–C} = 34 Hz, C₁ and C₂ of 1,2-O₂C₆H₄), 134.9 (s, 6C, C_{ipso} of P(C₆H₅)₃), 134.0 (m, 12C,

C_{ortho} of P(C₆H₅)₃), 129.4 (m, 12C, C_{meta} of P(C₆H₅)₃), 119.9 (s, 4C, C₄ and C₅ of 1,2-O₂C₆H₄), 111.0 (s, 4C, C₃ and C₆ of 1,2-O₂C₆H₄) + toluene of solvation. These values are similar, but not identical, with those reported in ref 7a. Those authors have not reported ¹³C NMR data, nor did they observe the broad ¹¹B resonance for **3a** in the initial study. Anal. Calcd for C₄₈H₃₈B₂O₄P₂Pt·C₇H₈: C, 62.94; H, 4.42. Found: C, 62.61; H, 4.71.

***cis*–[(PPh₃)₂Pt(B(1,2-O₂-4-Bu^tC₆H₃))₂] (**3b**).** This compound was prepared similarly to compound **3a**: yield = 88%; mp 184.3–185.6 °C (dec, 137 °C); ³¹P{¹H} NMR δ 29.0 (br, J_{Pt–P} = 1621 Hz); ¹¹B{¹H} δ 50.1 (br); ¹H NMR δ 7.36 (m, 12H, P(C₆H₅)₃), 7.05 (m, 18H, P(C₆H₅)₃), 6.81 (t, J = 1.1 Hz, 2H, H₃ of (1,2-O₂-4-Bu^tC₆H₃)), 6.68 (2 coincidentally overlapped doublets, both with J = 1.1 Hz, 4H, H₆ and H₅ of (1,2-O₂-4-Bu^tC₆H₃)), 1.20 (s, 18H, C(CH₃)₃); ¹³C{¹H} NMR δ 150.5 (s, 2C, ³J_{Pt–C} = 35 Hz, C₂ of (1,2-O₂-4-Bu^tC₆H₃)), 148.4 (s, 2C, ³J_{Pt–C} = 35 Hz, C₁ of (1,2-O₂-4-Bu^tC₆H₃)), 143.4 (s, 2C, C₄ of (1,2-O₂-4-Bu^tC₆H₃)), 135.5 (d, 6C, ¹J_{P–C} = 44 Hz, ²J_{Pt–C} = 20 Hz, C_{ipso} of P(C₆H₅)₃), 134.0 (m, 12C, C_{ortho} of P(C₆H₅)), 129.4 (s, 6C, C_{para} of P(C₆H₅)), 127.7 (m, 12C, C_{meta} of P(C₆H₅)), 116.3 (s, 2C, C₅ of (1,2-O₂-4-Bu^tC₆H₃)), 109.8 (s, 2C, C₃ of (1,2-O₂-4-Bu^tC₆H₃)), 108.6 (s, 2C, C₆ of (1,2-O₂-4-Bu^tC₆H₃)), 34.3 (s, 2C, C(CH₃)₃), 31.7 (s, 2C, C(CH₃)₃). Anal. Calcd for C₅₆H₅₄B₂O₄P₂Pt: C, 62.88; H, 5.09. Found: C, 62.95; H, 5.16.

***cis*–[(PPh₃)₂Pt(B(OC(CH₃)₂C(CH₃)₂O))₂] (**3c**).** The compound [(PPh₃)₂Pt(η-C₂H₄)] (**4**; 212 mg, 0.284 mmol) and B₂(pin)₂ (**1c**; 72 mg, 0.284 mmol) were placed in a scintillation vial, and CDCl₃ (1 mL) was added. The solution was stirred at ambient temperature, and the slow evolution of ethylene gas was apparent. The reaction mixture was stirred overnight, resulting in a red solution which was analyzed by NMR spectroscopy: ³¹P{¹H} NMR δ 28.5 (br, J_{Pt–P} = 1504 Hz, **3c**), 26.5 (sh, J_{Pt–P} = 3189 Hz); ¹¹B{¹H} NMR δ ca. 50 (vbr, **3c**), 30.1 (**1c**), 21.4 (7).

Synthesis of *cis*–[(PP)Pt(Bcat)₂] Compounds (PP = dppe, dppb). *cis*–[(Ph₂PCH₂CH₂PPh₂)Pt(B(1,2-O₂C₆H₄))₂] (5a**).** Compound **3a** (250 mg, 0.261 mmol) was dissolved in toluene (5 mL), and dppe (104 mg, 0.261 mmol) was added as a toluene solution (3 mL) via pipet. The solution was stirred overnight, and a white precipitate formed, which was collected by filtration and dried *in vacuo*: yield 165 mg (76%); mp 225.0–226.8 °C (dec, 170 °C); ³¹P{¹H} NMR (C₆D₆/THF) δ 57.8 (J_{Pt–P} = 1454 Hz); ¹¹B{¹H} NMR (C₆D₆/THF) δ 48.9 (br); ¹H NMR δ 7.74 (m, 8H, P(C₆H₅)₃), 7.34 (m, 12H, P(C₆H₅)₃), 7.06 (m, 4H, 1,2-O₂C₆H₄), 6.84 (m, 4H, 1,2-O₂C₆H₄), 2.38 (dm, J = 17.5 Hz, 4H, PCH₂), ¹³C{¹H} NMR δ 150.0 (4C, C₁ and C₂ of (1,2-O₂C₆H₄)), 134.8 (br, s, 4C, C_{ipso} of P(C₆H₅)₃), 133.3 (m, 8C, C_{ortho} of P(C₆H₅)₃), 130.6 (4C, C_{para} of P(C₆H₅)₃), 128.6 (m, 8C, C_{meta} of P(C₆H₅)₃), 120.5 (4C, C₄ and C₅ of (1,2-O₂C₆H₄)), 111.3 (4C, C₃ and C₆ of (1,2-O₂C₆H₄)), 29.3 (m, 2C, CH₂). Anal. Calcd for C₃₈H₃₂B₂O₄P₂Pt: C, 54.90; H, 3.88. Found: C, 54.54; H, 3.66.

***cis*–[(Ph₂P(CH₂)₄PPh₂)Pt(B(1,2-O₂C₆H₄))₂] (**5b**).** This compound was prepared similarly to compound **5a**: yield 174 mg (77%); mp 209.3–210.3 °C (dec, 165 °C); ³¹P{¹H} NMR (C₆D₆/THF) δ 21.6 (J_{Pt–P} = 1589 Hz); ¹¹B{¹H} NMR (C₆D₆/THF) δ 48.9 (br); ¹H NMR δ 7.50 (m, 8H, P(C₆H₅)₃), 7.21 (m, 12H, P(C₆H₅)₃), 6.83 (m, 4H, 1,2-O₂C₆H₄), 6.72 (m, 4H, 1,2-O₂C₆H₄), 2.68 (br, s, 4H, P–CH₂), 1.84 (br, d, J = 20 Hz, 4H, P–CH₂CH₂); ¹³C{¹H} NMR δ 149.9 (s, 4C, ³J_{Pt–C} = 34 Hz, C₁ and C₂ of (1,2-O₂C₆H₄)), 135.9 (d, 4C, ¹J_{P–C} = 47 Hz, C_{ipso} of P(C₆H₅)₃), 132.7 (m, 8C, C_{ortho} of P(C₆H₅)₃), 129.7 (s, 4C, C_{para} of P(C₆H₅)₃), 128.1 (m, 8C, C_{meta} of P(C₆H₅)₃), 120.1 (s, 4C, C₄ and C₅ of (1,2-O₂C₆H₄)), 111.0 (s, 4C, C₃ and C₆ of (1,2-O₂C₆H₄)), 28.0 (m, 2C, P–CH₂), 23.9 (m, 2C, PCH₂CH₂). Anal. Calcd for C₄₀H₃₆B₂O₄P₂Pt: C, 55.91; H, 4.22. Found: C, 55.22; H, 4.03.

Synthesis of B₂(OC(CH₃)₂C(CH₃)₂O)₃ (7**).** A 1 M solution of BH₃ in THF (2.8 mL, 2.8 mmol) was added dropwise to a THF solution (15 mL) of HOC(CH₃)₂C(CH₃)₂OH (500 mg, 4.23 mmol), and the evolution of gas was apparent. The solution was stirred for 14 h and reduced *in vacuo*. The residue was dissolved in toluene and filtered through Celite. The filtrate

(29) (a) Nguyen, P.; Todd, S.; Van den Biggelaar, D.; Taylor, N. J.; Marder, T. B.; Wittmann, F.; Friend, R. H. *Synlett* **1994**, 299. (b) Nguyen, P.; Yuan, Z.; Agocs, L.; Lesley, G.; Marder, T. B. *Inorg. Chim. Acta* **1994**, *220*, 289.

(30) Nöth, H. *Z. Naturforsch.* **1984**, *39B*, 1463.

was reduced *in vacuo* and redissolved in CDCl_3 for analysis: ^1H NMR δ 1.23 (s, 24H), 1.37 (s, 12H); $^{13}\text{C}\{^1\text{H}\}$ NMR δ 81.9 (4C), 79.5 (2C), 24.5 (8C), 22.7 (4C); ^{11}B NMR δ 21.9.

Catalytic Synthesis of Bis(boronate esters). In a typical catalytic reaction, in an N_2 filled glovebox, a thick-walled tube capped with a Youngs stopcock was charged with alkyne **8a–h** or diyne **9a,b** (1.9×10^{-4} mol), diboron reagent **1a,c** (1.9×10^{-4} mol, or 3.8×10^{-4} mol for **9a,b**), catalyst **4** or **3b** (ca. 5.7×10^{-6} mol, 3 mol %), and toluene (5 mL). The tube was sealed and heated to 80°C , and aliquots (1 μL) were removed hourly to monitor the disappearance of alkyne via GC/MS. Upon completion, the toluene was removed *in vacuo*, and the crude product was analyzed by GC/MS and ^1H , $^{11}\text{B}\{^1\text{H}\}$, and $^{13}\text{C}\{^1\text{H}\}$ NMR spectroscopy (CDCl_3). All compounds containing the Bpin functional groups were stable under the GC/MS conditions, whereas those containing Bcat functional groups could not be observed in many cases due to decomposition in the injector or on the column. Observed isotope distributions for parent ions showed excellent agreement with calculated ones. For the GC/MS analysis of compounds **11h**, **16**, and **17–21** the relative intensities of the fragments with respect to the largest peak in the spectra are included. The values reported in amu for the fragments formed represent in each case the peak with the largest contribution to the surrounding isotopic pattern. In some instances the parent ions were not observed; however, in all of these cases the observed isotope distributions were in agreement with calculated ones for the parent ion minus one methyl group.

(E)-C₆H₁₃C(B(1,2-O₂C₆H₄))=CH(B(1,2-O₂C₆H₄)) (10a): ^1H NMR (500 MHz) δ 7.18 (m, 2H, (1,2-O₂C₆H₄)), 7.05 (m, 4H, (1,2-O₂C₆H₄)), 6.98 (m, 2H, (1,2-O₂C₆H₄)), 6.51 (s, 1H, C=CH), 2.56 (t, $J = 6.9$ Hz, 2H, =CCH₂), 1.58 (m, 2H, =CCH₂CH₂), 1.29 (m, 6H, CH₃(CH₂)₃), 0.89 (t, 3H, CH₃); $^{13}\text{C}\{^1\text{H}\}$ NMR (125 MHz) δ 156.7 (br, 1C, B–C), 148.14 (2C, C₁ and C₂ of (1,2-O₂C₆H₄)), 148.10 (2C, C₁ and C₂ of (1,2-O₂C₆H₄)), 129.7 (br, 1C, B–C), 122.7 (2C, C₄ and C₅ of (1,2-O₂C₆H₄)), 122.5 (2C, C₄ and C₅ of (1,2-O₂C₆H₄)), 112.4 (2C, C₃ and C₆ of (1,2-O₂C₆H₄)), 112.3 (2C, C₃ and C₆ of (1,2-O₂C₆H₄)), 39.8 (1C, C=C–CH₂), 31.6 (1C, =CCH₂CH₂), 28.9 (1C, =CCH₂CH₂CH₂), 28.7 (1C, CH₃–CH₂CH₂), 22.6 (1C, CH₃CH₂CH₂), 14.0 (1C, CH₃CH₂CH₂); $^{11}\text{B}\{^1\text{H}\}$ NMR (64 MHz) δ 31.7 (br, overlapped, 2B).

(E)-C₆H₅C(B(1,2-O₂C₆H₄))=CH(B(1,2-O₂C₆H₄)) (10b): ^1H NMR (200 MHz) δ 7.54 (m, 2H, C₆H₅), 7.30 (m, 3H, C₆H₅), 7.25 (m, 2H, (1,2-O₂C₆H₄)), 7.10 (m, 2H, (1,2-O₂C₆H₄)), 7.01 (s, 4H, (1,2-O₂C₆H₄)), 6.98 (s, 1H, C=CH); $^{13}\text{C}\{^1\text{H}\}$ NMR (50 MHz) δ 154.5 (br, 1C, B–C), 148.2 (2C, C₁ and C₂ of (1,2-O₂C₆H₄)), 147.9 (2C, C₁ and C₂ of (1,2-O₂C₆H₄)), 140.5 (1C, C₆H₅), 128.9 (1C, C₆H₅), 128.7 (2C, C₆H₅), 126.7 (2C, C₆H₅), 122.8 (2C, C₄ and C₅ of (1,2-O₂C₆H₄)), 122.6 (2C, C₄ and C₅ of (1,2-O₂C₆H₄)), 112.6 (2C, C₃ and C₆ of (1,2-O₂C₆H₄)), 112.3 (2C, C₃ and C₆ of (1,2-O₂C₆H₄)) (one C–B resonance not observed); $^{11}\text{B}\{^1\text{H}\}$ NMR (64 MHz) δ 31.4 (br, overlapped, 2B).

(E)-(4-MeO-C₆H₄)C(B(1,2-O₂C₆H₄))=CH(B(1,2-O₂-C₆H₄)) (10c): mp 108.7–109.8 $^\circ\text{C}$; ^1H NMR (200 MHz) δ 7.52 (d, $J = 8.8$ Hz, 2H, MeOC₆H₄), 7.30 (m, 2H, (1,2-O₂C₆H₄)), 7.16 (m, 2H, (1,2-O₂C₆H₄)), 6.98 (s, 4H, (1,2-O₂C₆H₄)), 6.90 (d, $J = 8.8$ Hz, 2H, MeOC₆H₄), 6.87 (s, 1H, C=CH), 3.81 (s, 3H, MeOC₆H₄); $^{13}\text{C}\{^1\text{H}\}$ NMR (50 MHz) δ 160.5 (1C, C₄ of MeOC₆H₄), 154.0 (br, B–C), 148.3 (2C, C₁ and C₂ of (1,2-O₂C₆H₄)), 148.0 (2C, C₁ and C₂ of (1,2-O₂C₆H₄)), 133.1 (1C, C₁ of MeOC₆H₄), 128.4 (2C, C₂ and C₆ of MeOC₆H₄), 124.0 (br, B–C), 122.9 (2C, C₄ and C₅ of (1,2-O₂C₆H₄)), 122.6 (2C, C₄ and C₅ of (1,2-O₂C₆H₄)), 114.2 (2C, C₃ and C₅ of MeOC₆H₄), 112.7 (2C, C₃ and C₆ of (1,2-O₂C₆H₄)), 112.3 (2C, C₃ and C₆ of (1,2-O₂C₆H₄)), 55.3 (OCH₃); $^{11}\text{B}\{^1\text{H}\}$ NMR (64 MHz) δ 32.0 (br, overlapped, 2B).

(E)-(4-NC-C₆H₄)C(B(1,2-O₂C₆H₄))=CH(B(1,2-O₂C₆H₄)) (10d): ^1H NMR (200 MHz) δ 7.70 (s, broad, 4H, NCC₆H₄), 7.26 (m, 2H, (1,2-O₂C₆H₄)), 7.17 (m, 2H, (1,2-O₂C₆H₄)), 7.08 (s, broad, 4H, (1,2-O₂C₆H₄)), 7.05 (s, 1H, C=CH); $^{13}\text{C}\{^1\text{H}\}$ NMR (50 MHz) δ 148.0 (2C, C₁ and C₂ of (1,2-O₂C₆H₄)), 147.9 (2C, C₁ and C₂ of (1,2-O₂C₆H₄)), 145.3 (1C, C₁ of NCC₆H₄), 132.6 (2C, C₃ and C₅ of NCC₆H₄), 127.7 (2C, C₂ and C₆ of NCC₆H₄),

123.2 (2C, C₄ and C₅ of (1,2-O₂C₆H₄)), 123.0 (2C, C₄ and C₅ of (1,2-O₂C₆H₄)), 118.7 (1C, C \equiv N), 112.8 (2C, C₃ and C₆ of (1,2-O₂C₆H₄)), 112.6 (2C, C₃ and C₆ of (1,2-O₂C₆H₄)), 112.3 (1C, C₄ of NCC₆H₄); $^{11}\text{B}\{^1\text{H}\}$ NMR (64 MHz) δ 31.5 (br, overlapped, 2B).

(Z)-(C₆H₅)C(B(1,2-O₂C₆H₄))=C(C₆H₅)(B(1,2-O₂C₆H₄)) (10e): mp 161.2–162.4 $^\circ\text{C}$; ^1H NMR (200 MHz) δ 7.18 (m, 10H, C₆H₅), 7.05 (m, 4H, (1,2-O₂C₆H₄)), 7.00 (m, 4H, (1,2-O₂C₆H₄)); $^{13}\text{C}\{^1\text{H}\}$ NMR (50 MHz) δ 148.0 (4C, C₁ and C₂ of (1,2-O₂C₆H₄)), 139.1 (2C, C=C), 129.2 (4C, C₆H₅), 128.2 (4C, C₆H₅), 127.1 (2C, C₆H₅), 122.8 (4C, C₄ and C₅ of (1,2-O₂C₆H₄)), 112.5 (4C, C₃ and C₆ of (1,2-O₂C₆H₄)) (C–B resonances too broad to observe); $^{11}\text{B}\{^1\text{H}\}$ NMR (64 MHz) δ 31.8. Anal. Calcd for C₂₆H₁₈B₂O₄: C, 75.06; H, 4.36. Found: C, 75.21; H, 4.50.

(Z)-(4-Me-C₆H₄)C(B(1,2-O₂C₆H₄))=C(4-Me-C₆H₄)(B(1,2-O₂C₆H₄)) (10f): mp 197.8–198.6 $^\circ\text{C}$; ^1H NMR (C₆D₆, 250 MHz) δ 7.22 (d, $J = 8.0$ Hz, 4H, MeC₆H₄), 6.89 (m, 4H, (1,2-O₂C₆H₄)), δ 6.83 (d, $J = 8.0$ Hz, 4H, MeC₆H₄), 6.73 (m, 4H, (1,2-O₂C₆H₄)), 1.98 (s, 6H, MeC₆H₄); $^{13}\text{C}\{^1\text{H}\}$ NMR (50 MHz) δ 148.2 (4C, C₁ and C₂ of (1,2-O₂C₆H₄)), 136.9 (2C, C₄ of 4-MeC₆H₄), 136.3 (2C, C₁ of 4-MeC₆H₄), 129.3 (4C, C₂ and C₆ of MeC₆H₄), 129.0 (4C, C₃ and C₅ of MeC₆H₄), 122.7 (4C, C₄ and C₅ of (1,2-O₂C₆H₄)), 112.5 (4C, C₃ and C₆ of (1,2-O₂C₆H₄)), 21.2 (2C, CH₃C₆H₄) (C–B resonances too broad to observe); $^{11}\text{B}\{^1\text{H}\}$ NMR (64 MHz) δ 31.2.

(Z)-(4-MeO-C₆H₄)C(B(1,2-O₂C₆H₄))=C(4-MeO-C₆H₄)(B(1,2-O₂C₆H₄)) (10g): ^1H NMR (200 MHz) δ 7.13 (d, $J = 8.6$ Hz, 4H, MeOC₆H₄), 7.03 (m, 8H, (1,2-O₂C₆H₄)), 6.74 (d, $J = 8.6$ Hz, 4H, MeOC₆H₄), 3.70 (s, 6H, MeOC₆H₄); $^{13}\text{C}\{^1\text{H}\}$ NMR (50 MHz) δ 158.7 (2C, C₄ of MeOC₆H₄), 148.1 (4C, C₁ and C₂ of (1,2-O₂C₆H₄)), 144.3 (br, 2C, B–C), 131.6 (2C, C₁ of MeOC₆H₄), 130.7 (4C, C₂ and C₆ of MeOC₆H₄), 122.7 (4C, C₄ and C₅ of (1,2-O₂C₆H₄)), 113.7 (4C, C₃ and C₅ of MeOC₆H₄), 112.4 (4C, C₃ and C₆ of (1,2-O₂C₆H₄)), 55.0 (2C, CH₃O); $^{11}\text{B}\{^1\text{H}\}$ NMR (64 MHz) δ 31.8.

(E)-C₆H₁₃C(B(OC(CH₃)₂C(CH₃)₂O))=CH(B(OC(CH₃)₂C-(CH₃)₂O)) (11a): ^1H NMR (200 MHz) δ 5.85 (s, 1H, C=CH), 2.23 (t, $J = 6.2$ Hz, 2H, C=CCH₂), 1.40–1.20 (m, 8H, C=CCH₂-(CH₂)₄), 1.33 (s, 12H, (OC(CH₃)₂C(CH₃)₂O)), 1.23 (s, 12H, (OC(CH₃)₂C(CH₃)₂O)), 0.88 (t, $J = 6.7$ Hz, 3H, CH₃); $^{13}\text{C}\{^1\text{H}\}$ NMR (50 MHz) δ 83.2 (2C, (OC(CH₃)₂C(CH₃)₂O)), 82.8 (2C, (OC(CH₃)₂C(CH₃)₂O)), 39.6 (C=CCH₂), 31.4 (C=CCH₂CH₂), 28.8 (C=CCH₂CH₂CH₂), 28.3 (CH₃CH₂CH₂), 24.6 (8C, overlapped, (OC(CH₃)₂C(CH₃)₂O)), 22.7 (CH₃CH₂), 13.7 (CH₃) (C–B resonances too broad to observe); $^{11}\text{B}\{^1\text{H}\}$ NMR (64 MHz) δ 30.7 (br, overlapped, 2B); MS (EI) m/z 364 amu (M^+ for $^{12}\text{C}_{20}^{13}\text{H}_{38}^{11}\text{B}_2^{16}\text{O}_4$).

(E)-C₆H₅C(B(OC(CH₃)₂C(CH₃)₂O))=CH(B(OC(CH₃)₂C-(CH₃)₂O)) (11b): ^1H NMR (250 MHz) δ 7.43 (m, 2H, C₆H₅), 7.28 (m, 3H, C₆H₅), 6.29 (s, 1H, C=CH), 1.37 (s, 12H, (OC(CH₃)₂C(CH₃)₂O)), 1.30 (s, 12H, (OC(CH₃)₂C(CH₃)₂O)); $^{13}\text{C}\{^1\text{H}\}$ NMR (50 MHz) δ 142.8 (1C, C₆H₅), 128.1 (2C, C₆H₅), 127.4 (1C, C₆H₅), 126.3 (2C, C₆H₅), 83.9 (2C, (OC(CH₃)₂C(CH₃)₂O)), 83.2 (2C, (OC(CH₃)₂C(CH₃)₂O)), 24.9 (4C, (OC(CH₃)₂C(CH₃)₂O)), 24.7 (4C, (OC(CH₃)₂C(CH₃)₂O)) (C–B resonances too broad to observe); $^{11}\text{B}\{^1\text{H}\}$ NMR (64 MHz) δ 30.2 (br, overlapped, 2B); MS (EI) m/z 356 amu (M^+ for $^{12}\text{C}_{20}^{13}\text{H}_{30}^{11}\text{B}_2^{16}\text{O}_4$).

(E)-(4-MeO-C₆H₄)C(B(OC(CH₃)₂C(CH₃)₂O))=CH(B(OC(CH₃)₂C-(CH₃)₂O)) (11c): ^1H NMR (250 MHz) δ 7.39 (d, $J = 8.6$ Hz, 2H, MeOC₆H₄), 6.84 (d, $J = 8.6$ Hz, 2H, MeOC₆H₄), 6.21 (s, 1H, C=CH), 3.79 (s, 3H, CH₃O), 1.33 (s, 12H, (OC(CH₃)₂C(CH₃)₂O)), 1.30 (s, 12H, (OC(CH₃)₂C(CH₃)₂O)); $^{13}\text{C}\{^1\text{H}\}$ NMR (50 MHz) δ 159.3 (1C, C₄ of MeOC₆H₄), 135.4 (1C, C₁ of MeOC₆H₄), 127.7 (2C, C₂ and C₆ of MeOC₆H₄), 113.6 (2C, C₃ and C₅ of MeOC₆H₄), 83.9 (2C, (OC(CH₃)₂C(CH₃)₂O)), 83.3 (2C, (OC(CH₃)₂C(CH₃)₂O)), 55.0 (CH₃O), 25.0 (4C, (OC(CH₃)₂C-(CH₃)₂O)), 24.8 (4C, (OC(CH₃)₂C(CH₃)₂O)) (C–B resonances too broad to observe); $^{11}\text{B}\{^1\text{H}\}$ NMR (64 MHz) δ 30.2 (br, overlapped, 2B); MS (EI) m/z 386 amu (M^+ for $^{12}\text{C}_{21}^{13}\text{H}_{32}^{11}\text{B}_2^{16}\text{O}_5$).

(E)-(4-NC-C₆H₄)C(B(OC(CH₃)₂C(CH₃)₂O))=CH(B(OC(CH₃)₂C-(CH₃)₂O)) (11d): ^1H NMR (200 MHz) δ 7.59 (d, $J = 8.3$ Hz, 2H, NCC₆H₄), 7.51 (d, $J = 8.3$ Hz, 2H, NCC₆H₄), 6.37 (s, 1H, C=CH), 1.37 (s, 12H, (OC(CH₃)₂C(CH₃)₂O)), 1.32 (s,

12H, (OC(CH₃)₂C(CH₃)₂O)); ¹³C{¹H} NMR (50 MHz) δ 147.7 (1C, C₁ of NCC₆H₄), 132.1 (2C, C₃ and C₅ of NCC₆H₄), 127.2 (2C, C₂ and C₆ of NCC₆H₄), 119.0 (1C, C≡N), 110.0 (1C, C₄ of NCC₆H₄), 84.4 (2C, (OC(CH₃)₂C(CH₃)₂O)), 83.9 (2C, (OC(CH₃)₂C(CH₃)₂O)), 24.8 (4C, (OC(CH₃)₂C(CH₃)₂O)), 24.5 (4C, (OC(CH₃)₂C(CH₃)₂O)) (C–B resonances too broad to observe); ¹¹B{¹H} NMR (64 MHz) δ 30.9 (br, overlapped, 2B); MS (EI) *m/z* 381 amu (M⁺ for ¹²C₂₁¹H₂₉¹¹B₂¹⁴N¹⁶O₄).

(Z)-(C₆H₅)C(B(OC(CH₃)₂C(CH₃)₂O))=C(C₆H₅)(B(OC(CH₃)₂C(CH₃)₂O)) (11e): ¹H NMR (200 MHz) δ 7.05 (m, 6H, C₆H₅), 6.94 (d, *J* = 6.8 Hz, 4H, C₆H₅), 1.32 (s, 24H, (OC(CH₃)₂C(CH₃)₂O)); ¹³C{¹H} NMR (50 MHz), 141.3 (2C, C=C), 129.3 (4C, C₆H₅), 127.4 (2C, C₆H₅), 125.8 (4C, C₆H₅), 84.1 (4C, (OC(CH₃)₂C(CH₃)₂O)), 24.9 (8C, (OC(CH₃)₂C(CH₃)₂O)) (C–B resonances too broad to observe); ¹¹B{¹H} NMR (64 MHz) δ 30.6; MS (EI) *m/z* 432 amu (M⁺ for ¹²C₂₆¹H₃₄¹¹B₂¹⁶O₄).

(Z)-(4-Me-C₆H₄)C(B(OC(CH₃)₂C(CH₃)₂O))=C(4-Me-C₆H₄)(B(OC(CH₃)₂C(CH₃)₂O)) (11f): ¹H NMR (200 MHz) δ 6.86 (m, 8H overlapping, MeC₆H₄), 2.22 (s, 6H, CH₃C₆H₄), 1.31 (s, 24H, (OC(CH₃)₂C(CH₃)₂O)); ¹³C{¹H} NMR (50 MHz) δ 138.3 (2C, C₄ of MeC₆H₄), 135.1 (2C, C₁ of MeC₆H₄), 129.2 (4C, C₂ and C₆ of MeC₆H₄), 128.2 (4C, C₃ and C₅ of MeC₆H₄), 83.9 (4C, (OC(CH₃)₂C(CH₃)₂O)), 24.9 (8C, (OC(CH₃)₂C(CH₃)₂O)), 54.9 (2C, CH₃C₆H₄); ¹¹B{¹H} NMR (64 MHz) δ 31.2; MS (EI) *m/z* 460 amu (M⁺ for ¹²C₂₈¹H₃₈¹¹B₂¹⁶O₄).

(Z)-(4-MeO-C₆H₄)C(B(OC(CH₃)₂C(CH₃)₂O))=C(4-MeO-C₆H₄)(B(OC(CH₃)₂C(CH₃)₂O)) (11g): mp 176.6–177.3 °C; ¹H NMR (200 MHz) δ 6.89 (d, *J* = 8.8 Hz, 4H, MeOC₆H₄), 6.62 (d, *J* = 8.8 Hz, 4H, MeOC₆H₄), 3.68 (s, 6H, CH₃O), 1.32 (s, 24H, (OC(CH₃)₂C(CH₃)₂O)); ¹³C{¹H} NMR (50 MHz) 157.6 (2C, C₄ of MeOC₆H₄), 144.9 (br, 2C, B–C), 133.8 (2C, C₁ of MeOC₆H₄), 130.6 (4C, C₂ and C₆ of MeOC₆H₄), 113.4 (4C, C₃ and C₅ of MeOC₆H₄), 83.9 (4C, (OC(CH₃)₂C(CH₃)₂O)), 54.9 (2C, CH₃O), 24.9 (8C, (OC(CH₃)₂C(CH₃)₂O)); ¹¹B{¹H} NMR (64 MHz) δ 30.5; MS (EI) *m/z* 492 amu (M⁺ for ¹²C₂₈¹H₃₈¹¹B₂¹⁶O₆). Anal. Calcd for C₂₈H₃₈B₂O₆: C, 68.32; H, 7.78. Found: C, 68.31; H, 7.86.

(Me₃Si)C(B(OC(CH₃)₂C(CH₃)₂O))=C(SiMe₃)(B(OC(CH₃)₂C(CH₃)₂O)) (11h): MS (EI) *m/z* (relative intensity) 424 amu (M⁺ for ¹²C₂₀¹H₄₂¹¹B₂¹⁶O₄²⁸Si₂, 1.6), 409 (5.1), 225 (1.9), 209 (1.5), 167 (3.1), 155 (3.3), 143 (2.4), 135 (1.0), 125 (2.5), 109 (1.8), 101 (2.5), 84 (100), 75 (3.6), 69 (14.4), 55 (7.2).

(Z)-(4-MeO-C₆H₄)C(B(OC(CH₃)₂C(CH₃)₂O))=C(B(OC(CH₃)₂C(CH₃)₂O))C(H)=CH(C₆H₅) (13a): ¹H NMR (200 MHz) δ 7.58 (d, *J* = 8.7 Hz, 2H, ≡CC₆H₄), 7.23 (d, *J* = 8.7 Hz, 2H, ≡CC₆H₄), 6.88 (d, *J* = 8.7 Hz, 2H, ≡CC₆H₄), 6.76 (d, *J* = 8.7 Hz, 2H, ≡CC₆H₄), 3.80 (s, 3H, CH₃O), 3.75 (s, 3H, CH₃O), 1.37 (s, 12H, (OC(CH₃)₂C(CH₃)₂O)), 1.31 (s, 12H, (OC(CH₃)₂C(CH₃)₂O)); ¹³C{¹H} NMR (50 MHz), δ 159.2 (1C, C₄ of MeOC₆H₄), 158.7 (1C, C₄ of MeOC₆H₄), 133.7 (1C, C₁ of MeOC₆H₄), 133.0 (2C, C₂ and C₆ of MeOC₆H₄), 130.1 (2C, C₂ and C₆ of MeOC₆H₄), 116.5 (1C, C₁ of MeOC₆H₄), 113.6 (2C, C₃ and C₅ of MeOC₆H₄), 112.8 (2C, C₃ and C₅ of MeOC₆H₄), 97.1 (C≡C), 89.6 (C≡C), 84.1 (2C, (OC(CH₃)₂C(CH₃)₂O)), 84.0 (2C, (OC(CH₃)₂C(CH₃)₂O)), 55.1 (CH₃O), 55.0 (CH₃O), 24.8 (4C, (OC(CH₃)₂C(CH₃)₂O)), 24.7 (4C, (OC(CH₃)₂C(CH₃)₂O)) (C–B resonances too broad to observe); ¹¹B{¹H} NMR (64 MHz) δ 31.3 (br, overlapped, 2B); MS (EI) *m/z* 516 amu (M⁺ for ¹²C₃₀¹H₃₈¹¹B₂¹⁶O₆).

(Z)-(Me₃Si)C(B(OC(CH₃)₂C(CH₃)₂O))=CB(OC(CH₃)₂C(CH₃)₂O))=C(SiMe₃) (13b): ¹H NMR (200 MHz) δ 1.34 (s, 12H, (OC(CH₃)₂C(CH₃)₂O)), 1.31 (s, 12H, (OC(CH₃)₂C(CH₃)₂O)), 0.29 (s, 9H, Si(CH₃)₃), 0.20 (s, 9H, Si(CH₃)₃); ¹³C{¹H} NMR (50 MHz) δ 107.9 (1C, C≡C), 102.8 (1C, C≡C), 84.2 (2C, (OC(CH₃)₂C(CH₃)₂O)), 83.6 (2C, (OC(CH₃)₂C(CH₃)₂O)), 25.4 (4C, (OC(CH₃)₂C(CH₃)₂O)), 24.6 (4C, (OC(CH₃)₂C(CH₃)₂O)), –0.3 (3C, Si(CH₃)₃), –0.6 (3C, Si(CH₃)₃) (C–B resonances too broad to observe); ¹¹B{¹H} NMR (64 MHz) δ 28.9 (br, overlapped, 2B); MS (EI) *m/z* 448 amu (M⁺ for ¹²C₂₂¹H₄₂¹¹B₂¹⁶O₄²⁸Si₂).

(Z,Z)-(4-MeO-C₆H₄)C(B(1,2-O₂C₆H₄))=C(B(1,2-O₂C₆H₄))C(B(1,2-O₂C₆H₄))=C(4-Me-OC₆H₄)(B(1,2-O₂C₆H₄)) (14a): mp 233.9–234.8 °C; ¹H NMR (200 MHz) δ 7.27 (d, *J* = 8.7 Hz, 4H, MeOC₆H₄), 7.00 (br s, 8H, (1,2-O₂C₆H₄)), 6.93 (br s, 8H,

(1,2-O₂C₆H₄)), 6.65 (d, *J* = 8.7 Hz, 4H, MeOC₆H₄), 3.61 (s, 6H, CH₃O); ¹³C{¹H} NMR (50 MHz) δ 159.5 (2C, C₄ of MeOC₆H₄), 148.1 (8C, C₁ and C₂ of (1,2-O₂C₆H₄)), 132.7 (2C, C₁ of MeOC₆H₄), 130.9 (4C, C₂ and C₆ of MeOC₆H₄), 122.7 (4C, C₄ and C₅ of (1,2-O₂C₆H₄)), 122.2 (4C, C₄ and C₅ of (1,2-O₂C₆H₄)), 113.9 (4C, C₃ and C₅ of MeOC₆H₄), 112.5 (4C, C₃ and C₆ of (1,2-O₂C₆H₄)), 111.9 (4C, C₃ and C₆ of (1,2-O₂C₆H₄)), 55.1 (2C, CH₃O) (C–B resonances too broad to observe); ¹¹B{¹H} NMR (64 MHz) δ 30.7 (br, overlapped, 4B). Anal. Calcd for C₄₂H₃₀B₄O₁₀: C, 68.36; H, 4.10. Found: C, 68.56; H, 4.22.

(Z,Z)-(4-MeO-C₆H₄)C(B(OC(CH₃)₂C(CH₃)₂O))=C(B(OC(CH₃)₂C(CH₃)₂O))C(B(OC(CH₃)₂C(CH₃)₂O))=C(4-MeO-C₆H₄)(B(OC(CH₃)₂C(CH₃)₂O)) (15a): ¹H NMR (200 MHz) δ 7.19 (d, *J* = 8.7 Hz, 4H, MeOC₆H₄), 6.73 (d, *J* = 8.7 Hz, 4H, MeOC₆H₄), 3.73 (s, 6H, CH₃O), 1.29 (s, 12H, (OC(CH₃)₂C(CH₃)₂O)), 1.25 (s, 12H, (OC(CH₃)₂C(CH₃)₂O)), 1.00 (s, 12H, (OC(CH₃)₂C(CH₃)₂O)), 0.95 (s, 12H, (OC(CH₃)₂C(CH₃)₂O)); ¹³C{¹H} NMR (50 MHz) δ 157.9 (2C, C₄ of MeOC₆H₄), 147.1 (B–C), 142.2 (B–C), 137.7 (2C, C₁ of MeOC₆H₄), 130.0 (4C, C₂ and C₆ of MeOC₆H₄), 112.9 (4C, C₃ and C₅ of MeOC₆H₄), 83.0 (4C, (OC(CH₃)₂C(CH₃)₂O)), 82.9 (4C, (OC(CH₃)₂C(CH₃)₂O)), 55.1 (CH₃O), 25.2 (4C, (OC(CH₃)₂C(CH₃)₂O)), 24.8 (4C, (OC(CH₃)₂C(CH₃)₂O)), 24.5 (4C, (OC(CH₃)₂C(CH₃)₂O)), 24.3 (4C, (OC(CH₃)₂C(CH₃)₂O)); ¹¹B{¹H} NMR (64 MHz) δ 30.0 (br, overlapped, 4B); MS (electrospray) 771 amu (M + H⁺ for ¹²C₄₂¹H₆₂¹¹B₄¹⁶O₁₀).

(Z,Z)-(Me₃Si)C(B(OC(CH₃)₂C(CH₃)₂O))=C(B(OC(CH₃)₂C(CH₃)₂O))C(B(OC(CH₃)₂C(CH₃)₂O))=C(SiMe₃)(B(OC(CH₃)₂C(CH₃)₂O)) (15b): MS (electrospray) 703 amu (M + H⁺ for ¹²C₃₄¹H₆₆¹¹B₄¹⁶O₈²⁸Si₂).

C₆H₅C≡CC(H)=CH(C₆H₅) (16): configuration unknown; MS (EI) *m/z* (relative intensity) 204 (100) amu (M⁺ for ¹²C₁₆¹H₁₂), 189 (6.4), 176 (5.5), 165 (4.5), 150 (3.3), 139 (2.0), 126 (9.2), 115 (1.2), 101 (15.4), 89 (6.3), 76 (6.9), 63 (4.4), 51 (6.9).

C₆H₅C(B(OC(CH₃)₂C(CH₃)₂O))=C(B(OC(CH₃)₂C(CH₃)₂O))C(H)=CH(C₆H₅) (17): configuration unknown; MS (EI) *m/z* (relative intensity) 458 (5.6) amu (M⁺ for ¹²C₂₈¹H₃₆¹¹B₂¹⁶O₄), 400 (2.6), 358 (5.6), 330 (20.6), 315 (3.3), 301 (9.5), 275 (25.8), 257 (31.7), 241 (4.8), 231 (39.9), 213 (49.8), 204 (100), 187 (6.0), 167 (3.3), 155 (9.8), 129 (11.6), 115 (4.6), 101 (12.1), 84 (57.9), 69 (31.0), 55 (24.7).

Me₃SiB(OC(CH₃)₂C(CH₃)₂O) (18): MS (EI) *m/z* (relative intensity) 185 (12.2) amu (M⁺ – ¹²C¹H₃ for ¹²C₉¹H₂₁¹¹B¹⁶O₂²⁸Si), 157 (3.4), 143 (6.9), 125 (2.5), 117 (4.7), 101 (20.9), 84 (100), 75 (20.7), 73 (15.0), 69 (56.0), 55 (10.0).

Me₃Si-C≡C-B(OC(CH₃)₂C(CH₃)₂O) (19): MS (EI) *m/z* (relative intensity) 224 (19.6) amu (M⁺ for ¹²C₁₁¹H₂₁¹¹B¹⁶O₂²⁸Si), 209 (70.6), 195 (3.3), 181 (6.9), 167 (52.4), 149 (22.1), 139 (32.1), 125 (100), 117 (5.6), 109 (46.5), 103 (8.2), 97 (22.7), 93 (14.5), 85 (20.7), 83 (27.4), 75 (27.4), 73 (21.7), 67 (12.7), 55 (11.7).

(Me₃Si)C(B(OC(CH₃)₂C(CH₃)₂O))=C(B(OC(CH₃)₂C(CH₃)₂O))₂ (20): MS (EI) *m/z* (relative intensity) 463 (1.4) amu (M⁺ – ¹²C¹H₃ for ¹²C₂₃¹H₄₅¹¹B₃¹⁶O₆²⁸Si), 420 (0.8), 363 (0.8), 337 (6.1), 295 (5.5), 280 (1.9), 254 (1.3), 237 (8.7), 221 (2.2), 197 (2.2), 181 (3.9), 167 (1.3), 153 (2.8), 143 (1.7), 135 (2.4), 125 (1.7), 109 (3.2), 101 (5.1), 84 (100), 73 (15.7), 69 (23.0), 55 (16.8).

Me₃SiB(1,2-O₂C₆H₄) (21): MS (EI) *m/z* (relative intensity) 192 amu (M⁺ for ¹²C₉¹H₁₃¹¹B¹⁶O₂²⁸Si), 177 (100), 161 (1.1), 149 (6.3), 135 (36.8), 117 (3.5), 105 (3.4), 91 (20.2), 73 (9.4), 58 (17.4), 53 (3.5).

Catalytic Reactions Monitored by NMR Spectroscopy. In a typical catalytic NMR tube reaction, in an N₂-filled glovebox, an NMR tube was charged with 1-octyne (**8a**; 13 mg, 0.118 mmol), compound **1a** (31 mg, 0.130 mmol) or **1c** (33 mg, 0.130 mmol), and catalyst (**4**, 5 mg, ~5.7 mol %; **3b**, 6 mg, ~5 mol %, 6 × 10^{–6} mol). CDCl₃ was used to rinse the vials employed for weighing the reagents and then to top up the NMR tube up to a premeasured volume (0.5 mL). The tube was sealed and shaken and then placed in a warm water bath set to 52 °C for a period of 5 min and then in the spectrometer set at 52 °C for an additional 5 min. The ¹H NMR spectrum

Table 1. Data Collection and Structure Solution and Refinement for 3a,b and 5a,b

	3a	3b	5a	5b
formula	C ₄₈ H ₃₈ B ₂ O ₄ P ₂ Pt·C ₆ D ₆	C ₅₆ H ₅₄ B ₂ O ₄ P ₂ Pt	C ₃₈ H ₃₂ B ₂ O ₄ P ₂ Pt	C ₄₀ H ₃₆ B ₂ O ₄ P ₂ Pt
MW	1041.59	1069.64	831.29	859.34
cryst syst	triclinic	triclinic	triclinic	monoclinic
space group	<i>P</i> 1	<i>P</i> 1	<i>P</i> 1	<i>C</i> 2/ <i>c</i>
<i>a</i> (Å)	11.0771(10)	10.359(7)	10.9514(12)	15.655(2)
<i>b</i> (Å)	11.2471(10)	16.378(8)	12.1452(13)	10.4619(13)
<i>c</i> (Å)	20.909(2)	16.684(11)	13.4068(14)	22.305(3)
α (deg)	104.564(2)	102.19(4)	97.716(3)	90
β (deg)	90.118(2)	107.79(3)	108.341(3)	107.200(3)
γ (deg)	115.667(2)	106.85(3)	93.200(2)	90
<i>V</i> (Å ³)	2254.0(3)	2431(3)	1668.1(3)	3489.8(8)
<i>Z</i>	2	2	2	4
<i>d</i> _{calc} (g cm ⁻³)	1.535	1.461	1.655	1.636
cryst size (mm)	0.42 × 0.38 × 0.12	0.08 × 0.08 × 0.02	0.12 × 0.12 × 0.04	0.18 × 0.10 × 0.08
cryst color	pale yellow	colorless	yellow	colorless
temp (K)	160	160	160	160
μ (mm ⁻¹)	3.231	2.998	4.343	4.155
<i>F</i> (000)	1036	1080	820	1704
no. of rflns for cell refinement	8734 (θ range 2.0–25.5°)	45 (θ range 1.0–23.5°)	5629 (θ range 2.0–25.5°)	4820 (θ range 2.0–25.4°)
θ range, deg	2.03–25.52	1.58–25.41	1.62–25.46	1.91–25.55
index ranges	−13 ≤ <i>h</i> ≤ 13, −12 ≤ <i>k</i> ≤ 12, −24 ≤ <i>l</i> ≤ 18	−12 ≤ <i>h</i> ≤ 11, −19 ≤ <i>k</i> ≤ 14, −19 ≤ <i>l</i> ≤ 19	−13 ≤ <i>h</i> ≤ 8, −12 ≤ <i>k</i> ≤ 13, −15 ≤ <i>l</i> ≤ 15	−18 ≤ <i>h</i> ≤ 17, −12 ≤ <i>k</i> ≤ 10, −27 ≤ <i>l</i> ≤ 26
no. of rflns measd	9819	10 453	7234	7351
no. of indep rflns	7114 (<i>R</i> _{int} = 0.0383)	7592 (<i>R</i> _{int} = 0.0512)	5258 (<i>R</i> _{int} = 0.0443)	2913 (<i>R</i> _{int} = 0.0440)
no. of rflns with <i>I</i> > 2σ(<i>I</i>)	6918	6627	4927	2584
max and min transmissn	0.847, 0.525	0.832, 0.692	0.592, 0.498	0.550, 0.470
weighting params <i>a</i> , <i>b</i>	0.0373, 7.4975	0.0000, 29.5992	0.0649, 6.4357	0.0210, 45.1574
no. of params	569	602	425	233
GOF on <i>F</i> ²	1.072	1.189	1.078	1.128
final <i>R</i> indices (<i>I</i> > 2σ(<i>I</i>))	<i>R</i> 1 = 0.0326, w <i>R</i> 2 = 0.0833	<i>R</i> 1 = 0.0583, w <i>R</i> 2 = 0.1217	<i>R</i> 1 = 0.0416, w <i>R</i> 2 = 0.1050	<i>R</i> 1 = 0.0419, w <i>R</i> 2 = 0.0896
<i>R</i> indices (all data) ^a	<i>R</i> 1 = 0.0337, w <i>R</i> 2 = 0.0844	<i>R</i> 1 = 0.0729, w <i>R</i> 2 = 0.1364	<i>R</i> 1 = 0.0453, w <i>R</i> 2 = 0.1089	<i>R</i> 1 = 0.0493, w <i>R</i> 2 = 0.0937
extinction coeff	0.0014(2)	0	0.0021(4)	0.00023(5)
largest shift/esd	0.001	0.001	0.002	0.010
largest diff peak and hole (e Å ⁻³)	1.15, −1.67	1.31, −2.08	2.05, −2.31	1.11, −1.12

^a *R* = Σ(|*F*_o − *F*_c|)/Σ(*F*_o), *R*_w = {Σ[w(*F*_o² − *F*_c²)]/Σ[w(*F*_o²)]^{1/2}, and GOF = *S* = {Σ[w(*F*_o² − *F*_c²)]/(*n* − *p*)^{1/2} for *n* reflections and *p* parameters in the refinement.

Table 2. Selected Bond Lengths (Å) and Angles (deg) for 3a

Bond Lengths			
Pt(1)–B(1)	2.040(6)	B(1)–O(1)	1.408(6)
Pt(1)–B(2)	2.058(6)	B(1)–O(2)	1.416(7)
Pt(1)–P(1)	2.3543(12)	B(2)–O(3)	1.398(7)
Pt(1)–P(2)	2.3465(12)	B(2)–O(4)	1.408(7)
Bond Angles			
B(1)–Pt(1)–B(2)	77.1(2)	B(1)–Pt(1)–P(2)	90.7(2)
B(2)–Pt(1)–P(2)	167.6(2)	B(1)–Pt(1)–P(1)	160.1(2)
B(2)–Pt(1)–P(1)	85.3(2)	P(2)–Pt(1)–P(1)	107.14(4)
O(1)–B(1)–Pt(1)	130.5(4)	O(2)–B(1)–Pt(1)	121.4(4)
O(3)–B(2)–Pt(1)	126.4(4)	O(4)–B(2)–Pt(1)	125.2(4)
O(1)–B(1)–O(2)	108.1(4)	O(3)–B(2)–O(4)	108.4(5)

Table 3. Selected Bond Lengths (Å) and Angles (deg) for 3b

Bond Lengths			
Pt(1)–B(1)	2.045(11)	B(1)–O(1)	1.425(12)
Pt(1)–B(2)	2.046(13)	B(1)–O(2)	1.406(12)
Pt(1)–P(1)	2.344(3)	B(2)–O(3)	1.415(13)
Pt(1)–P(2)	2.353(3)	B(2)–O(4)	1.412(13)
Bond Angles			
B(1)–Pt(1)–B(2)	77.2(4)	B(1)–Pt(1)–P(1)	163.8(3)
B(2)–Pt(1)–P(1)	90.7(3)	B(1)–Pt(1)–P(2)	88.9(3)
B(2)–Pt(1)–P(2)	164.0(3)	P(2)–Pt(1)–P(1)	104.37(10)
O(1)–B(1)–Pt(1)	121.1(7)	O(2)–B(1)–Pt(1)	130.5(7)
O(3)–B(2)–Pt(1)	123.5(7)	O(4)–B(2)–Pt(1)	128.1(8)
O(1)–B(1)–O(2)	108.1(8)	O(3)–B(2)–O(4)	108.2(9)

Table 4. Selected Bond Lengths (Å) and Angles (deg) for 5a

Bond Lengths			
Pt(1)–B(1)	2.058(8)	B(1)–O(1)	1.416(9)
Pt(1)–B(2)	2.048(8)	B(1)–O(2)	1.421(9)
Pt(1)–P(1)	2.304(2)	B(2)–O(3)	1.415(10)
Pt(1)–P(2)	2.332(2)	B(2)–O(4)	1.387(9)
Bond Angles			
B(1)–Pt(1)–B(2)	81.0(3)	B(1)–Pt(1)–P(1)	167.8(2)
B(2)–Pt(1)–P(1)	89.4(2)	B(1)–Pt(1)–P(2)	103.8(2)
B(2)–Pt(1)–P(2)	174.2(2)	P(2)–Pt(1)–P(1)	85.36(6)
O(1)–B(1)–Pt(1)	121.8(5)	O(2)–B(1)–Pt(1)	130.6(5)
O(3)–B(2)–Pt(1)	125.5(5)	O(4)–B(2)–Pt(1)	125.5(5)
O(1)–B(1)–O(2)	107.5(6)	O(3)–B(2)–O(4)	108.8(6)

Table 5. Selected Bond Lengths (Å) and Angles (deg) for 5b

Bond Lengths			
Pt(1)–B(1)	2.031(8)	B(1)–O(1)	1.442(9)
Pt(1)–P(1)	2.339(2)	B(1)–O(2)	1.402(9)
Bond Angles			
B(1A)–Pt(1)–B(1)	76.5(4)	O(1)–B(1)–Pt(1)	126.3(5)
B(1)–Pt(1)–P(1A)	167.8(2)	O(1)–B(1)–O(2)	106.9(6)
B(1)–Pt(1)–P(1)	91.4(2)	O(2)–B(1)–Pt(1)	126.7(5)
P(1A)–Pt(1)–P(1)	100.72(9)		

Reaction of [(PPh₃)₂Pt(η-C₂H₄)] with B₂(1,2-O₂C₆H₄)₃.

A CDCl₃ or C₆D₆ (0.5 mL) solution of B₂(cat)₃ (**6**, 23 mg, 6.7 × 10⁻⁵ mol) was added via pipet to solid **4** (50 mg, 6.7 × 10⁻⁵ mol), and the resultant orange to deep red solutions were analyzed by NMR spectroscopy. In CDCl₃: ³¹P{¹H} NMR δ 29.9 (s, *J*_{Pt–P} = 3368 Hz), 28.8 (s, *J*_{Pt–P} = 3021 Hz), minor products (δ 26.5, 23.6, 14.7 ppm); ¹¹B{¹H} NMR δ 23.7 (sharp), 14.5 ppm (sharp, minor product, [B(cat)₂]⁻); ¹H NMR (hydride region) δ −16.3 ppm (t, *J*_{P–H} = 13 Hz; *J*_{Pt–H} = 1197 Hz). In C₆D₆ (a red insoluble oil formed at the base of the NMR tube): ³¹P{¹H} NMR δ 30.6 (s, *J*_{Pt–P} = 3061 Hz), 23.1 ppm (minor

was recorded every 5 min for the first 30 min and then every 30 min until at least 3 half-lives had been completed. The initial time at ambient temperature was assumed to be negligible in terms of the progress of the reaction, and the reaction time coordinate was corrected for the initial heating period and variables such as total acquisition time and the delay between collection of spectra. In reactions involving **5a,b** ca. 5 mol % of catalyst was used.

Table 6. Data Collection and Structure Solution and Refinement for 10c,e and 14a

	10c	10e	14a
formula	C ₂₁ H ₁₆ B ₂ O ₅	C ₂₆ H ₁₈ B ₂ O ₄	C ₄₂ H ₃₀ B ₄ O ₁₀
MW	370.0	416.02	737.90
cryst syst	monoclinic	triclinic	triclinic
space group	<i>P</i> 2 ₁ / <i>c</i>	<i>P</i> $\bar{1}$	<i>P</i> $\bar{1}$
<i>a</i> (Å)	16.3130(14)	9.8189(11)	9.9576(13)
<i>b</i> (Å)	12.8737(9)	11.1751(12)	12.720(2)
<i>c</i> (Å)	8.8296(8)	20.672(2)	15.041(2)
α (deg)	90	81.699(3)	85.500(3)
β (deg)	103.927(6)	82.609(2)	82.553(3)
γ (deg)	90	66.367(2)	77.231(4)
<i>V</i> (Å ³)	1799.8(3)	2050.0(4)	1839.8(4)
Z	4	4	2
<i>d</i> _{calc} (g cm ⁻³)	1.365	1.348	1.332
cryst size	0.24 {100} × 0.22 {110} × 0.24 {10 $\bar{1}$ }	0.54 × 0.40 × 0.34	0.32 × 0.22 × 0.20
cryst color	colorless	colorless	yellow
temp (K)	180	160	160
μ (mm ⁻¹)	0.095	0.088	0.093
<i>F</i> (000)	768	864	764
no. of rflns for cell refinement	25 (θ range 11.0–16.0)	7176 (θ range 2.0–25.5)	4892 (θ range 2.1–27.5)
θ range (deg)	2.0–26.0	1.00–25.47	1.37–28.42
index ranges	0 ≤ <i>h</i> ≤ 20, 0 ≤ <i>k</i> ≤ 15, –10 ≤ <i>l</i> ≤ 10	–11 ≤ <i>h</i> ≤ 11, –10 ≤ <i>k</i> ≤ 13, –21 ≤ <i>l</i> ≤ 24	–12 ≤ <i>h</i> ≤ 9, –16 ≤ <i>k</i> ≤ 16, –19 ≤ <i>l</i> ≤ –20
no. of rflns measd	3658	8902	11301
no. of indep rflns	3534 (<i>R</i> _{int} = 0.014)	6449 (<i>R</i> _{int} = 0.0289)	7905 (<i>R</i> _{int} = 0.0370)
no. of rflns with <i>I</i> > 2 σ (<i>I</i>)	2627 ^a	5999	5553
max and min transmissn	0.973, 0.960		
weighting params <i>a</i> , <i>b</i>		0.0297, 0.8126	0.0353, 0.6302
no. of params	270	578	508
GOF	2.35 on <i>F</i>	1.084 on <i>F</i> ²	1.052 on <i>F</i> ²
final <i>R</i> indices (<i>I</i> > 2 σ (<i>I</i>))	<i>R</i> = 0.0337, <i>R</i> _w = 0.0336 ^a	<i>R</i> 1 = 0.0352, <i>wR</i> 2 = 0.0863	<i>R</i> 1 = 0.0454, <i>wR</i> 2 = 0.0971
<i>R</i> indices (all data) ^b	<i>R</i> = 0.0446, <i>R</i> _w = 0.0342	<i>R</i> 1 = 0.0387, <i>wR</i> 2 = 0.0903	<i>R</i> 1 = 0.0754, <i>wR</i> 2 = 0.1208
extinction coeff	0.00109(7)	0.0098(7)	0.0066(9)
largest shift/esd	0.002	0.001	<0.001
largest diff peak and hole (e Å ⁻³)	0.22, –0.15	0.19, –0.15	0.22, –0.19

^a $[F > 6\sigma(F)]$. ^b For **10c**, $R = \sum ||F_o| - |F_c|| / \sum (|F_o|)$, $R_w = \{\sum w(|F_o| - |F_c|)^2 / \sum [wF_o^2]\}^{1/2}$, and $GOF = S = \{\sum [w(|F_o| - |F_c|)^2] / (n - p)\}^{1/2}$; for **10e** and **14a**, see definition in Table 1.

Table 7. Selected Bond Lengths (Å) and Angles (deg) for 10c

Bond Lengths			
C(1)–C(2)	1.348(2)	B(9)–O(10)	1.388(2)
C(2)–C(3)	1.484(2)	B(9)–O(11)	1.392(2)
C(1)–B(9)	1.526(2)	B(18)–O(19)	1.386(2)
C(2)–B(18)	1.566(2)	B(18)–O(20)	1.386(2)
Bond Angles			
C(2)–C(1)–B(9)	124.4(1)	C(1)–C(2)–C(3)	123.6(1)
C(1)–C(2)–B(18)	120.1(1)	C(3)–C(2)–B(18)	116.3(1)
C(1)–B(9)–O(10)	124.6(1)	C(2)–B(18)–O(19)	123.0(2)
C(1)–B(9)–O(11)	124.5(1)	C(2)–B(18)–O(20)	125.5(2)
O(10)–B(9)–O(11)	110.9(1)	O(19)–B(18)–O(20)	111.4(1)

product); ¹¹B{¹H} NMR δ 22.4 (sharp), 15 ppm (minor); ¹H NMR (hydride region) δ –23.2 (t, *J*_{P–H} = 13.7 Hz; *J*_{Pt–H} = 1359 Hz).

X-ray Crystallography. Crystal data and other information on structure determination are given in Table 1 for the platinum complexes **3a,b** and **5a,b** and in Table 6 for the bis- and tetrakis(boronate esters) **10c,e** and **14a**. Measurements for **10c** were made on a Siemens P4 four-circle diffractometer and for the other samples on a Siemens SMART CCD area-detector diffractometer; in all cases, graphite-monochromated Mo K α radiation was used (λ = 0.710 73 Å). Crystals were obtained by diffusion of a layer of hexanes into a CDCl₃ solution for **5a,b** and **10c**, into a C₆D₆ solution for **3a**, and into a THF solution for **14a** and by slow evaporation of a CDCl₃ solution for **3b**. For all except **10c**, the crystals were mounted on a glass fiber with a coating of perfluoro polyether oil, cell parameters were refined from the observed setting angles and detector spot positions for selected reflections, and intensities were measured from a series of frames each covering a 0.3° oscillation in ω . The crystal of **10c** was mounted on a glass fiber with epoxy cement, cell parameters were refined from the observed setting angles of selected reflections, and intensities were measured with ω scans. Absorption corrections were

Table 8. Selected Bond Lengths (Å) and Angles (deg) for 10e

molecule 1		molecule 2	
Bond Lengths			
C(1)–C(2)	1.353(2)	C(51)–C(52)	1.358(2)
C(1)–B(1)	1.559(2)	C(51)–B(3)	1.553(2)
C(2)–B(2)	1.551(2)	C(52)–B(4)	1.562(2)
C(1)–C(31)	1.500(2)	C(51)–C(81)	1.491(2)
C(2)–C(41)	1.500(2)	C(52)–C(91)	1.497(2)
B(1)–O(1)	1.386(2)	B(3)–O(5)	1.390(2)
B(1)–O(2)	1.389(2)	B(3)–O(6)	1.384(2)
B(2)–O(3)	1.386(2)	B(4)–O(7)	1.381(2)
B(2)–O(4)	1.393(2)	B(4)–O(8)	1.388(2)
Bond Angles			
C(2)–C(1)–C(31)	121.64(13)	C(81)–C(51)–C(52)	121.43(14)
C(2)–C(1)–B(1)	126.51(14)	C(52)–C(51)–B(3)	119.28(14)
C(31)–C(1)–B(1)	111.84(12)	C(81)–C(51)–B(3)	119.29(13)
C(1)–C(2)–C(41)	121.32(13)	C(51)–C(52)–C(91)	123.58(14)
C(1)–C(2)–B(2)	121.72(14)	C(51)–C(52)–B(4)	125.23(14)
C(41)–C(2)–B(2)	116.91(13)	C(91)–C(52)–B(4)	111.03(12)

semiempirical for the platinum complexes, based on sets of equivalent reflections measured at different azimuthal angles; for **10c**, a face-indexed correction was applied, and no absorption corrections were made for **10e** and **14a**.

The structures were solved by heavy-atom (**3a,b**) and direct (all others) methods and refined by full-matrix least-squares techniques. For **10c** the refinement was on *F* using reflections with $F_o > 6\sigma(F_o)$, to minimize $\sum w(|F_o| - |F_c|)^2$, with weighting $w^{-1} = \sigma^2(F_o)$; the refined isotropic extinction parameter χ is defined such that F_c is multiplied by $(1 + 0.002\chi F_c^2 / (\sin 2\theta))^{-1/4}$. For the other structures, the refinement was on *F*² of all independent reflections, to minimize $\sum w(F_o^2 - F_c^2)^2$, with weighting $w^{-1} = \sigma^2(F_o^2) + (aP)^2/bP$, where $P = (F_o^2 + 2F_c^2)/3$; the refined isotropic extinction parameter χ is defined such that F_c is multiplied by $(1 + 0.001\chi F_c^2 / (\sin 2\theta))^{-1/4}$. In each case, anisotropic displacement parameters were refined for all

Table 9. Selected Bond Lengths (Å) and Angles (deg) for 14a

Bond Lengths			
C(1)–C(2)	1.373(3)	C(1)–C(31)	1.486(3)
C(1)–B(1)	1.541(3)	C(2)–C(3)	1.488(3)
C(2)–B(2)	1.570(3)	C(3)–C(4)	1.362(2)
C(3)–B(3)	1.565(3)	C(4)–C(61)	1.494(2)
C(4)–B(4)	1.546(3)	B(1)–O(1)	1.389(3)
B(1)–O(2)	1.389(2)	B(2)–O(3)	1.385(2)
B(2)–O(4)	1.389(2)	B(3)–O(6)	1.382(2)
B(3)–O(7)	1.393(2)	B(4)–O(8)	1.386(2)
B(4)–O(9)	1.384(2)		
Bond Angles			
C(2)–C(1)–C(31)	120.0(2)	C(2)–C(1)–B(1)	119.3(2)
C(31)–C(1)–B(1)	120.7(2)	C(1)–C(2)–C(3)	121.9(2)
C(1)–C(2)–B(2)	119.4(2)	C(3)–C(2)–B(2)	118.5(2)
C(4)–C(3)–C(2)	121.2(2)	C(4)–C(3)–B(3)	121.7(2)
C(2)–C(3)–B(3)	116.8(2)	C(3)–C(4)–C(61)	120.7(2)
C(3)–C(4)–B(4)	122.8(2)	C(61)–C(4)–B(4)	116.4(2)

non-hydrogen atoms, and isotropic hydrogen atoms were constrained to ride on their parent carbon atoms with fixed bond lengths and idealized bond angles.

In the case of **3b**, 2-fold disorder was resolved and refined for one *tert*-butyl group. Similarly, disorder was modeled for the backbone of the phosphine ligand in **5b**. In **5b**, the Pt atom is constrained to lie on a crystallographic C_2 axis. The structure of **10e** has two independent molecules in the asymmetric unit. Programs were standard Siemens control and integration software, versions 4 and 5 of SHELXTL,³¹ and local programs.

(31) Sheldrick, G. M. SHELXTL Siemens Analytical X-ray Instruments Inc., Madison, WI, 1990 and 1994.

Refined atomic coordinates and equivalent isotropic displacement parameters are given in the Supporting Information, and selected bond lengths and angles for the structures are given in Tables 2–5 for the platinum complexes and in Tables 7–9 for the bis- and tetrakis(boronate esters).

Acknowledgment. T.B.M. thanks the NSERC of Canada for research funding and Johnson Matthey Ltd. and E. I. du Pont de Nemours & Co., Inc., for generous supplies of platinum salts, N.C.N. and W.C. thank the EPSRC for support, G.L. and P.N. thank the British Council (Ottawa) for a travel scholarship, P.N. thanks the NSERC for a postgraduate scholarship, A.J.S. thanks the EPSRC for a studentship, and T.B.M. and N.C.N. thank the NSERC, The Royal Society (London), and the University of Newcastle-upon-Tyne for supporting this collaboration through a series of travel grants. We also thank Prof. S. Collins for the preliminary molecular mechanics calculations, Mr. L. E. B. Taylor for assistance with the electrospray MS studies, and Profs. J. F. Hartwig and M. R. Smith III for communication of results prior to publication.

Supporting Information Available: Complete lists of bond lengths and angles, anisotropic displacement parameters, hydrogen atom parameters, and non-hydrogen atom parameters for **3a,b**, **5a,b**, **10c,e**, and **14a** (45 pages). Ordering information is given on any current masthead page. Also, these data have been deposited at the Cambridge Crystallographic Data Centre.

OM950918C